Supporting Information

Melanogenesis-Inhibitory and Cytotoxic Activities of Triterpene Glycoside Constituents from the Bark of *Albizia procera*

Jie Zhang,[†,‡] Toshihiro Akihisa,[⊥] Masahiro Kurita,[⊥] Takashi Kikuchi,[|] Wan-Fang Zhu,[†] Feng Ye,[†] Zhen-Huan Dong,[▽] Wen-Yuan Liu,[▽] Feng Feng[*,†,‡,§] and Jian Xu,[*†]

[†]Department of Natural Medicine Chemistry, China Pharmaceutical University, 24 Tongjiaxiang, Nanjing 210009, China

[‡]Key Laboratory of Biomedical Functional Materials, China Pharmaceutical University, Nanjing 211198, China

[§]Jiangsu Food and Pharmaceutical Science College, Huaian, Jiangsu, 223003, China

[⊥] College of Science and Technology, Nihon University, 1-8-14 Kanda Surugadai, Chiyoda-ku, Tokyo 101-8308, Japan

[|] Osaka University of Pharmaceutical Sciences, Nasahara, Takatsuki, Osaka 569-1094, Japan

[▽] Department of Pharmaceutical Analysis, China Pharmaceutical University, Nanjing 210009, China

S1. IR spectrum of proceraoside E (**1**)

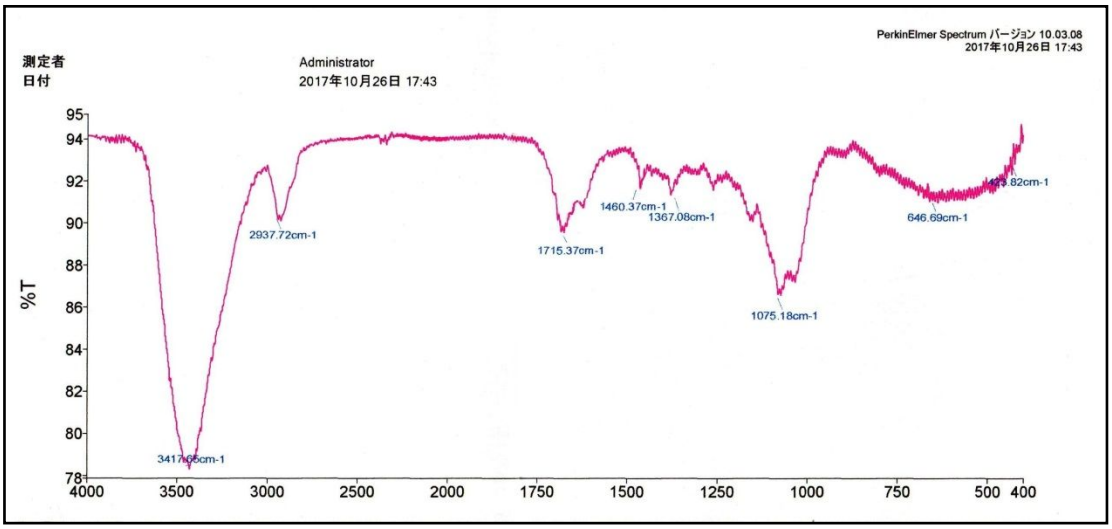

S2. UV spectrum of proceraoside E (**1**)

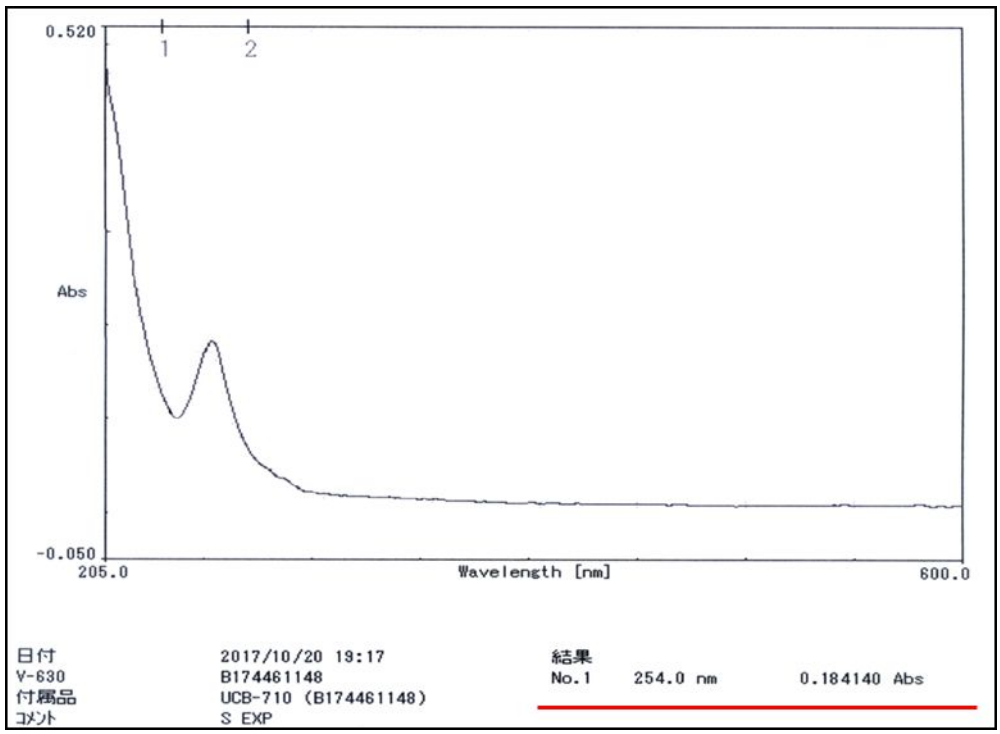

S3. ^{1}H NMR spectrum of proceraoside E (**1**)

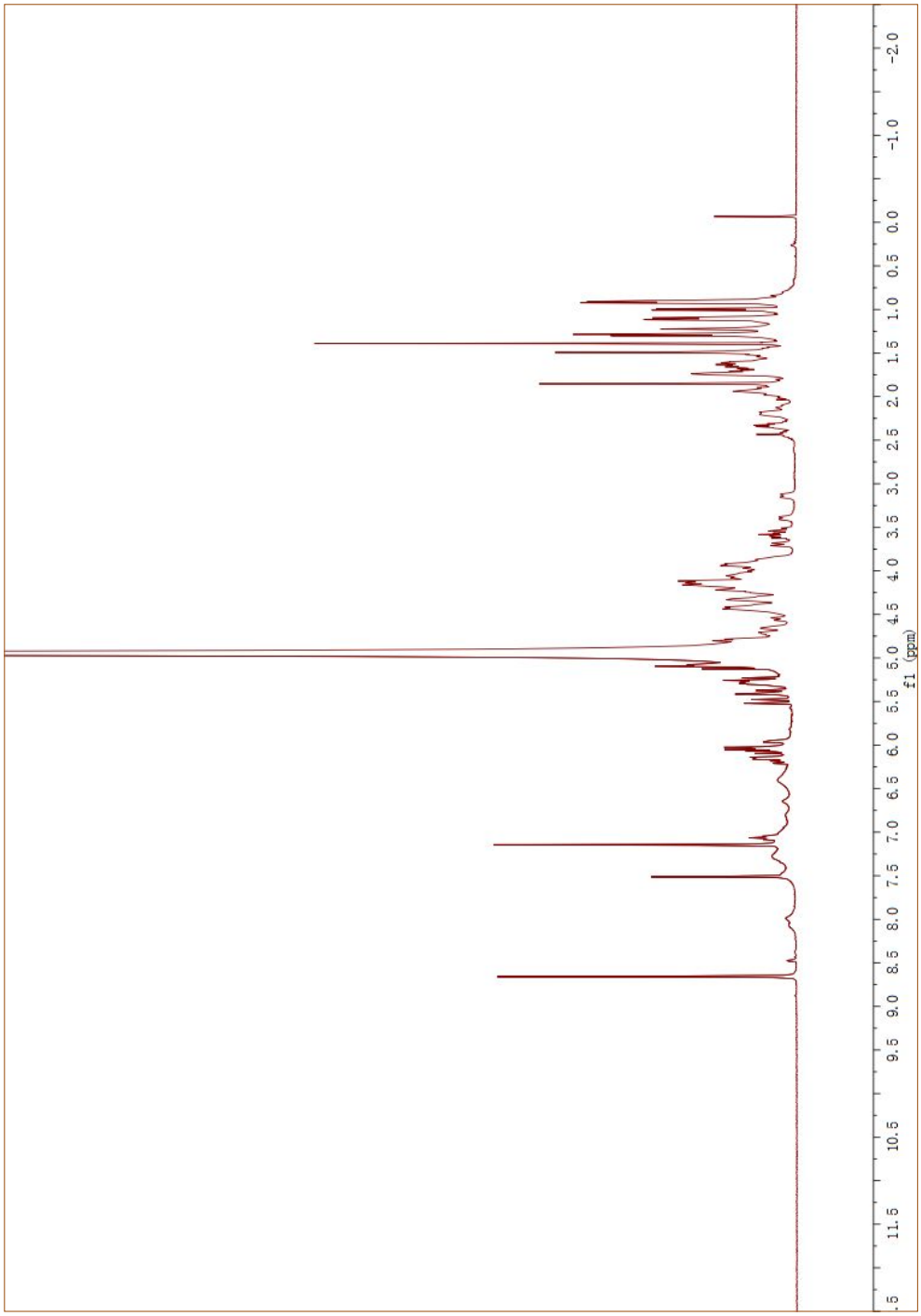
f1 (ppm)

S4. ^{13}C NMR spectrum of proceraoside E (**1**)

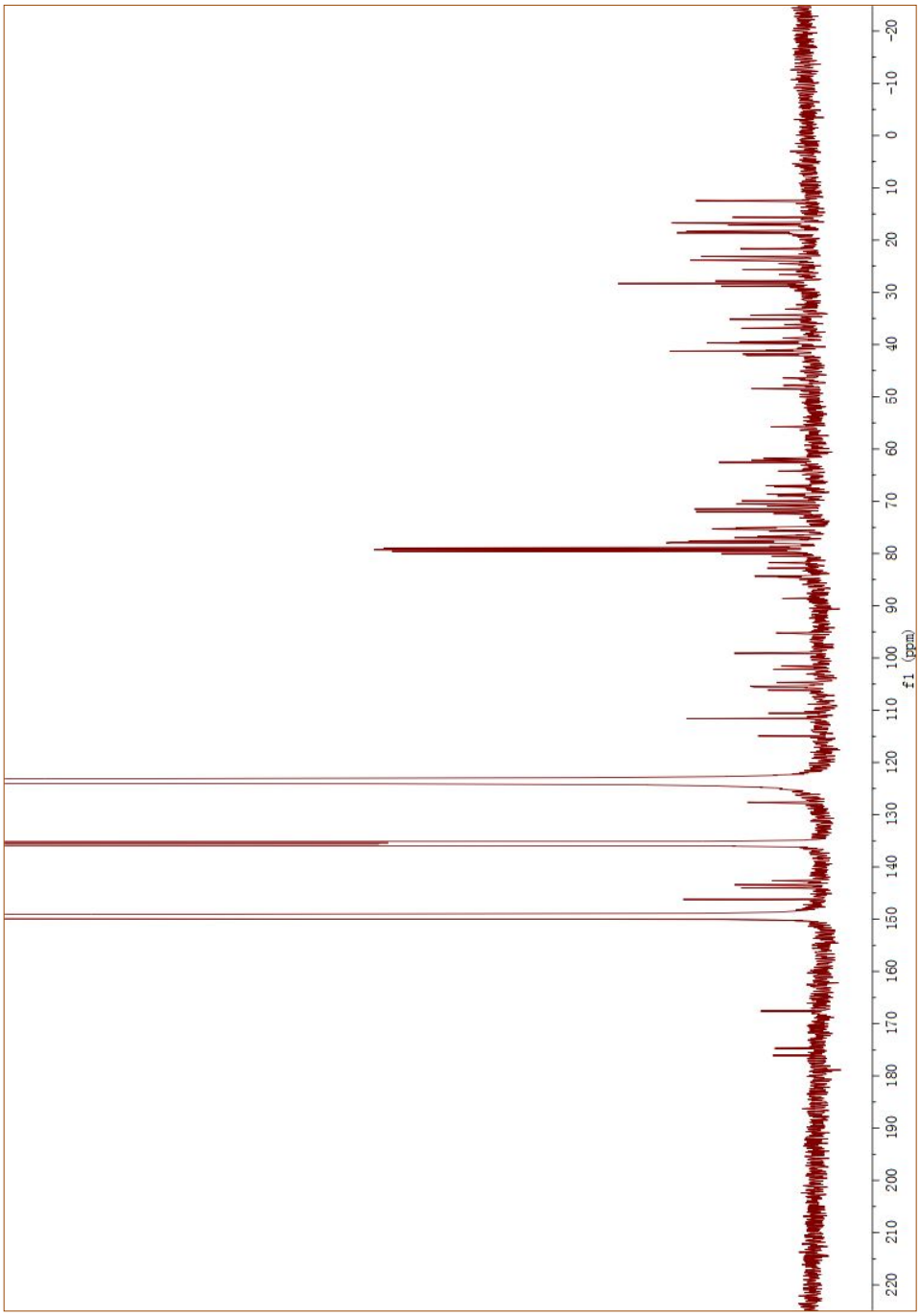

S5. H-H COSY spectrum of proceraoside E (**1**)

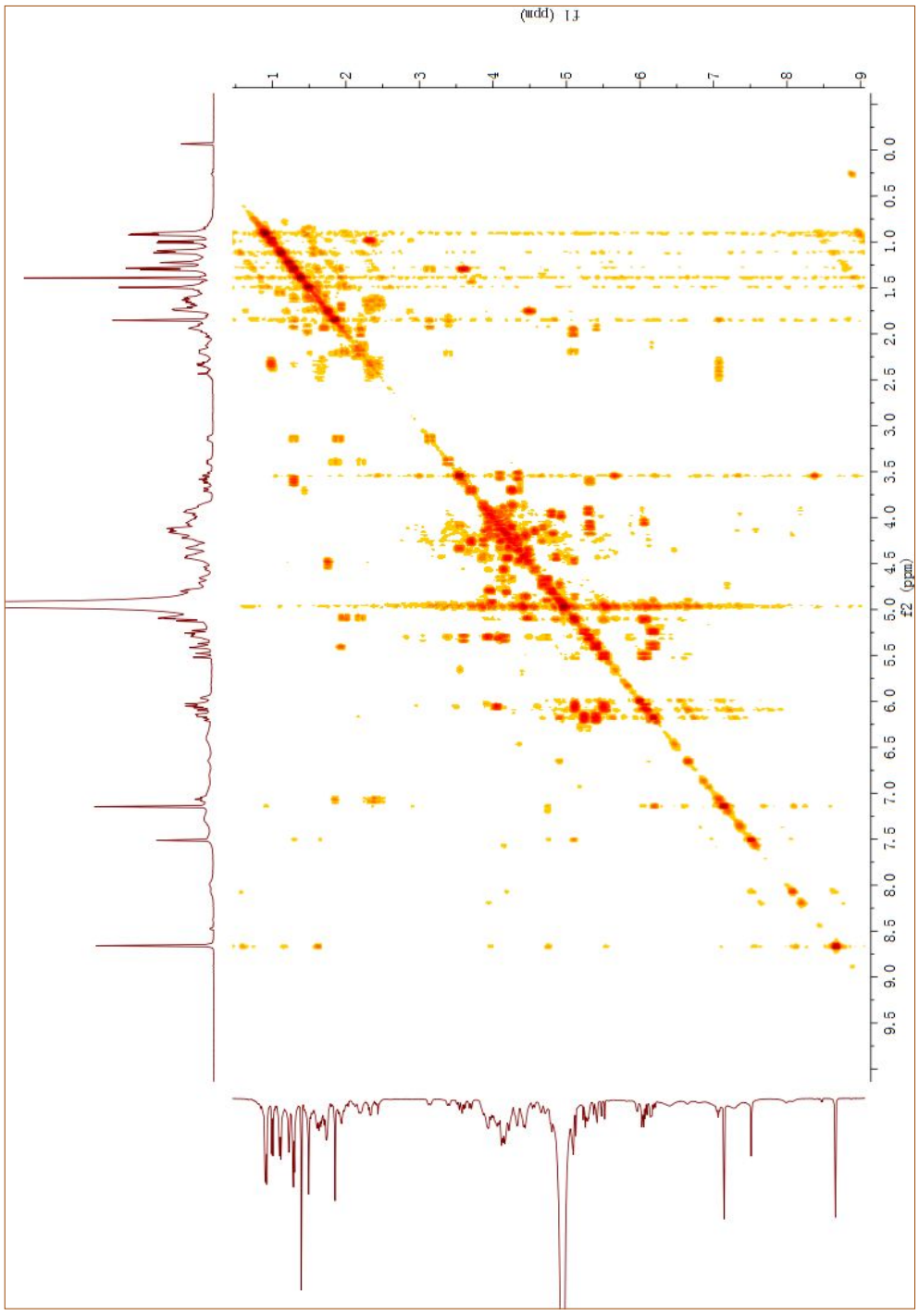

S6. HMQC spectrum of proceraoside E (**1**)

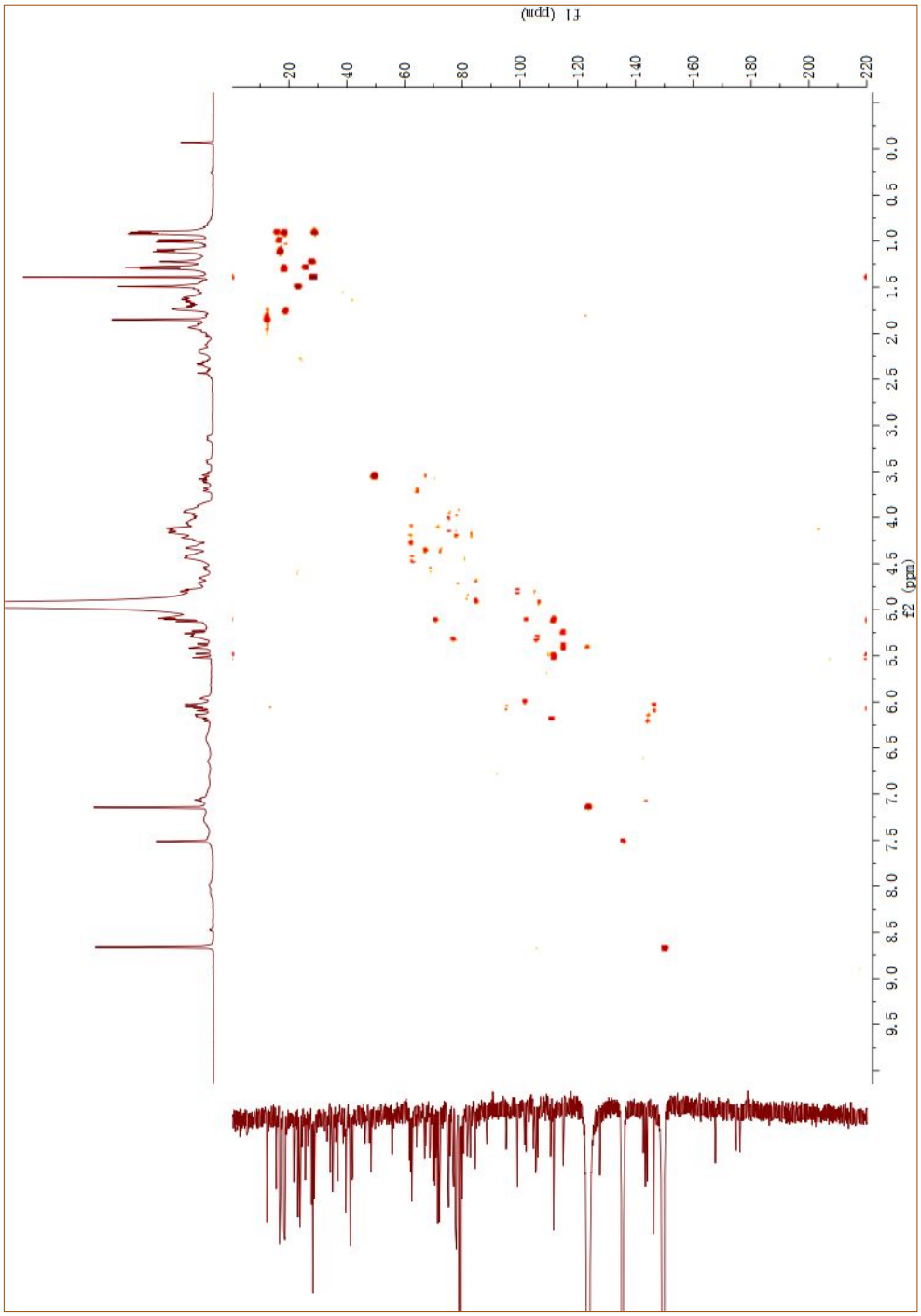

S7. HMBC spectrum of proceraoside E (**1**)

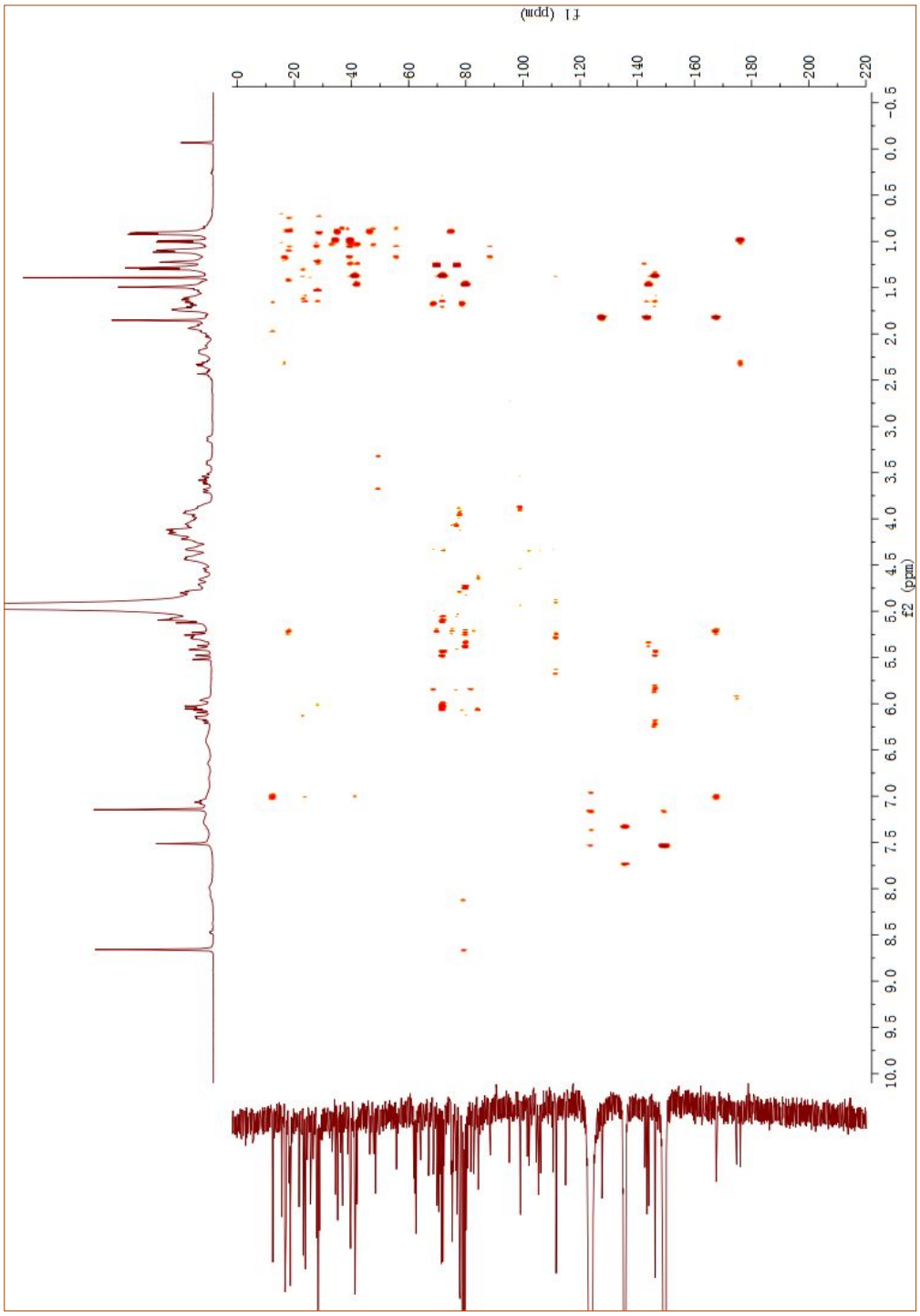

S8. NOSEY spectrum of proceraoside E (**1**)

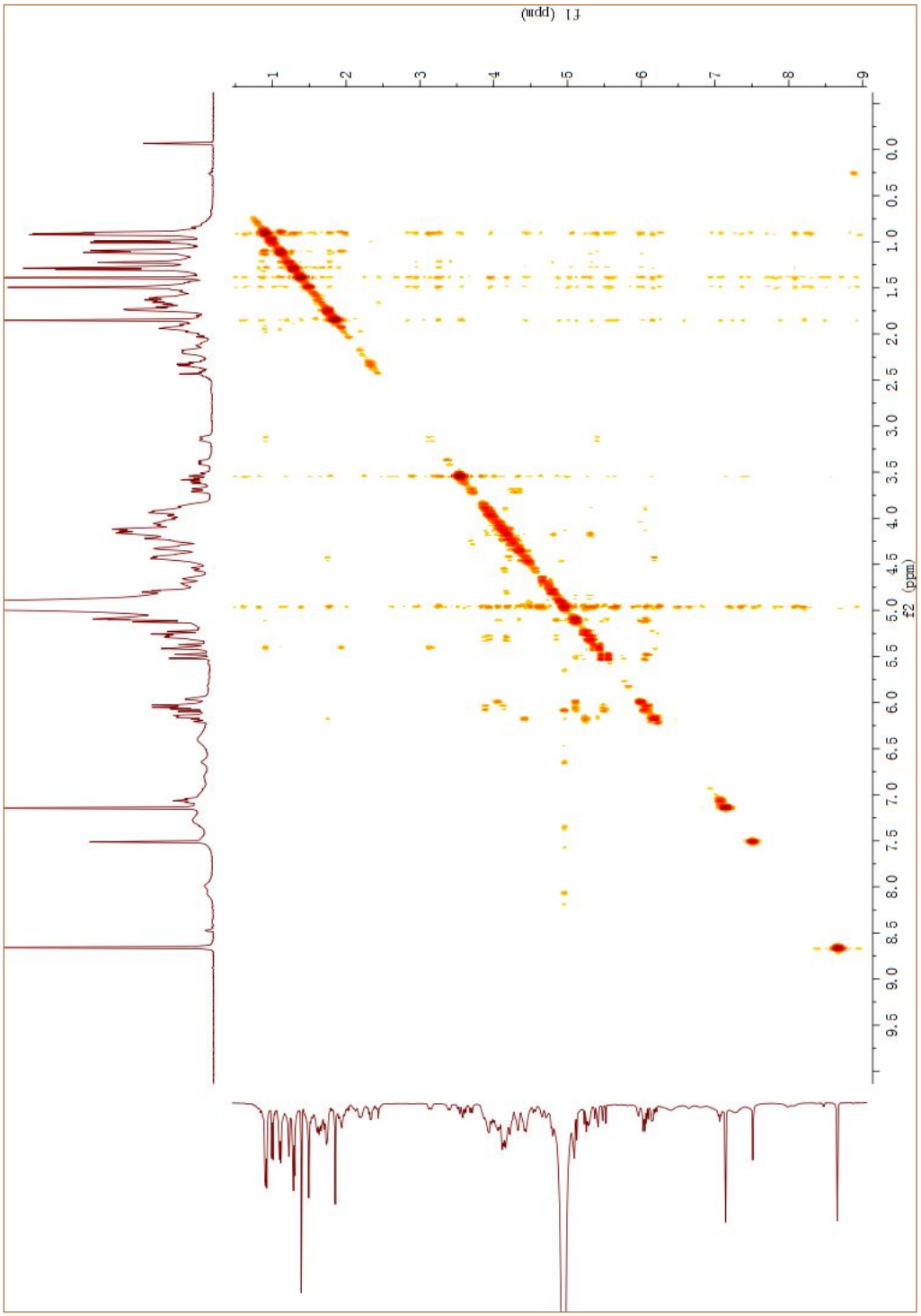

S9. HRESIMS spectrum of proceraoside E (**1**)

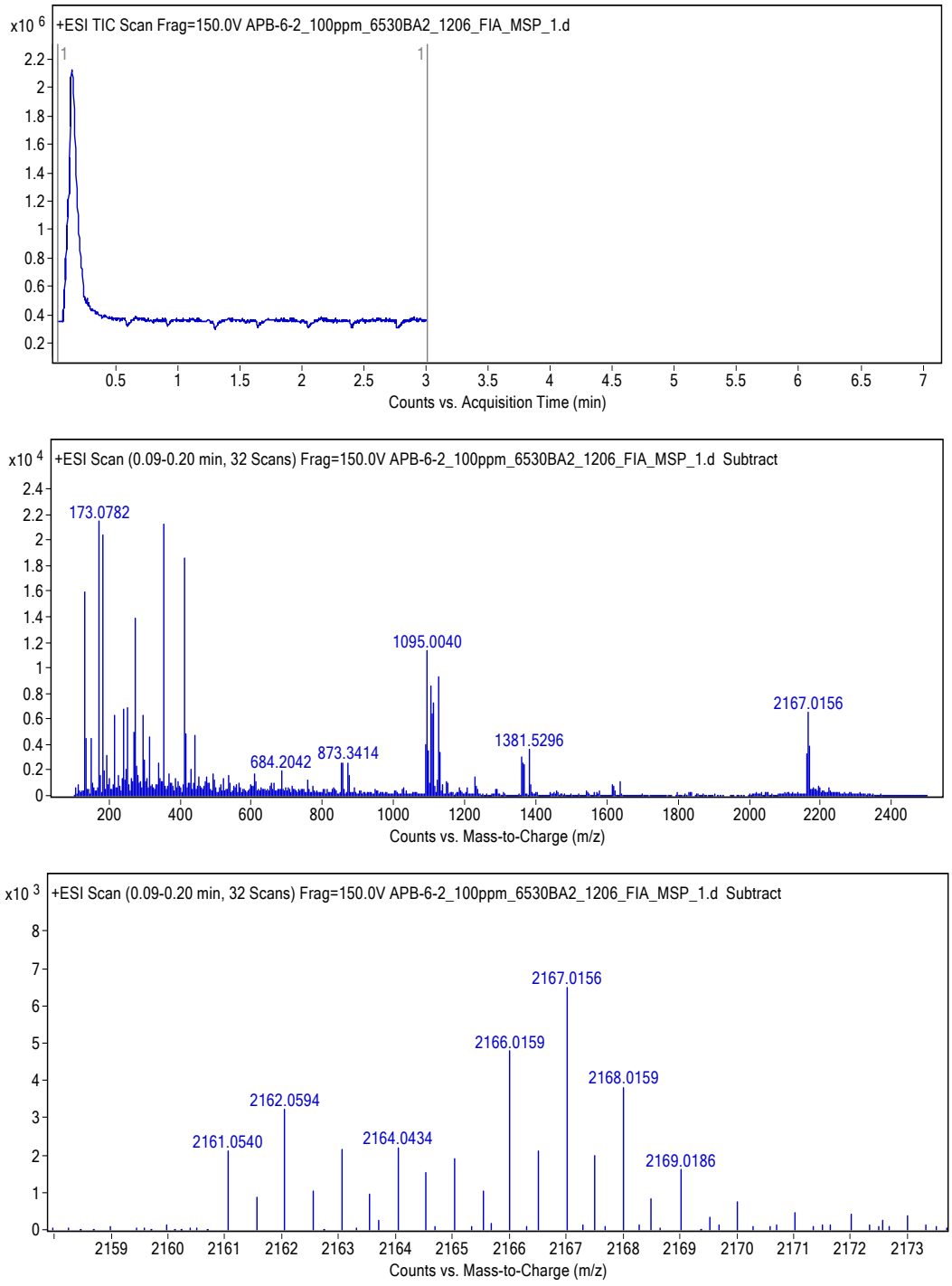

S10. IR spectrum of proceraoside F (**2**)

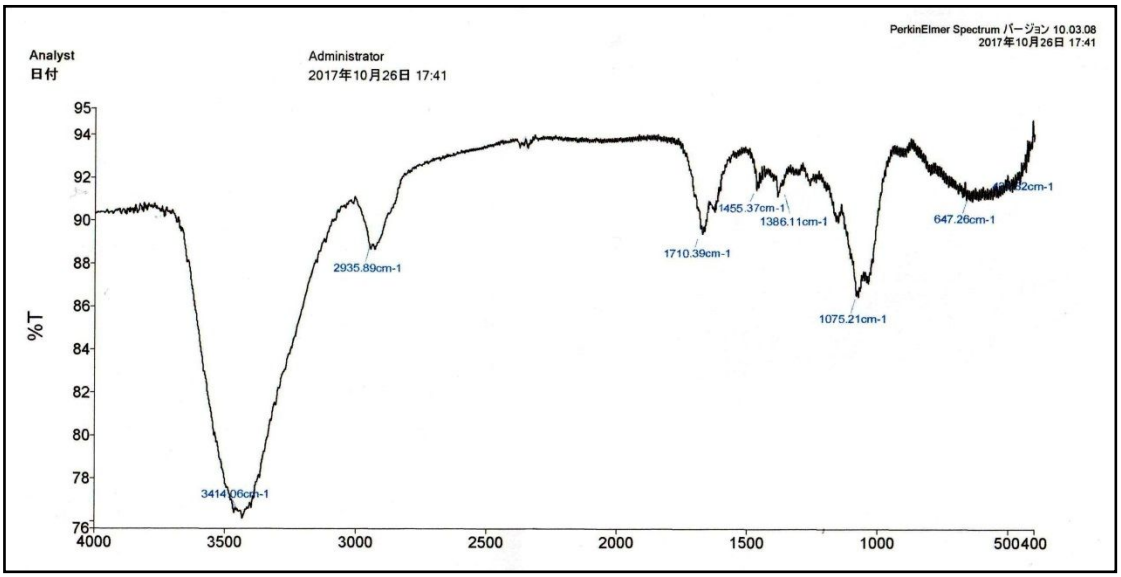

S11. UV spectrum of proceraoside F (**2**)

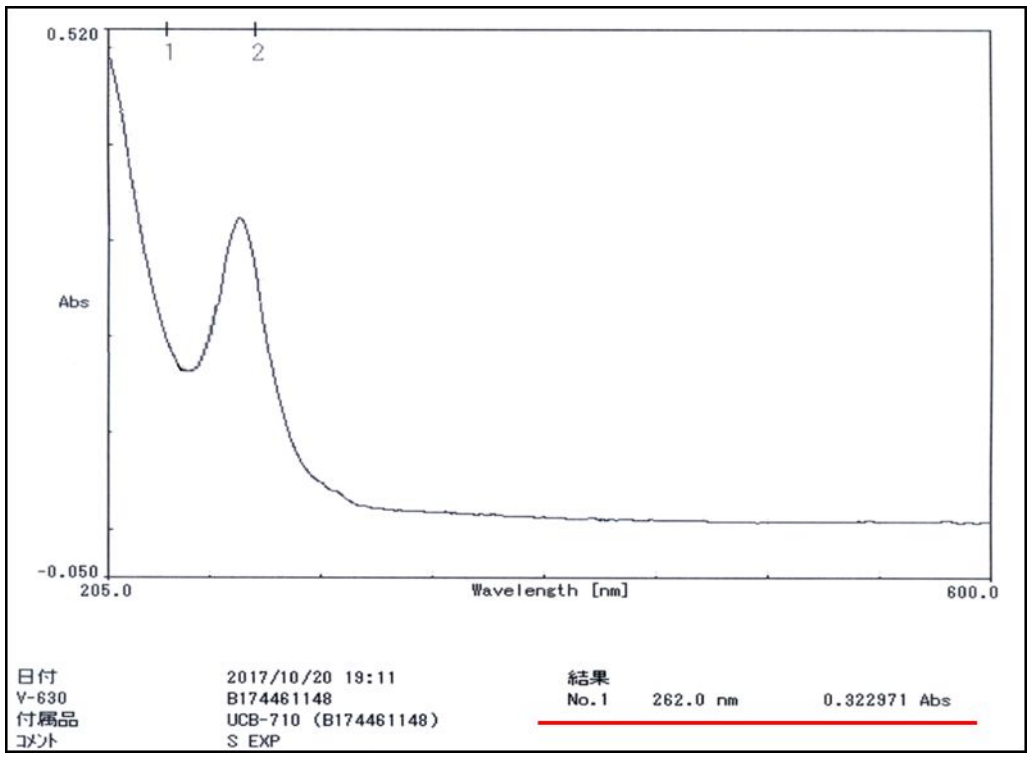

S12. ^{1}H NMR spectrum of proceraoside F (**2**)

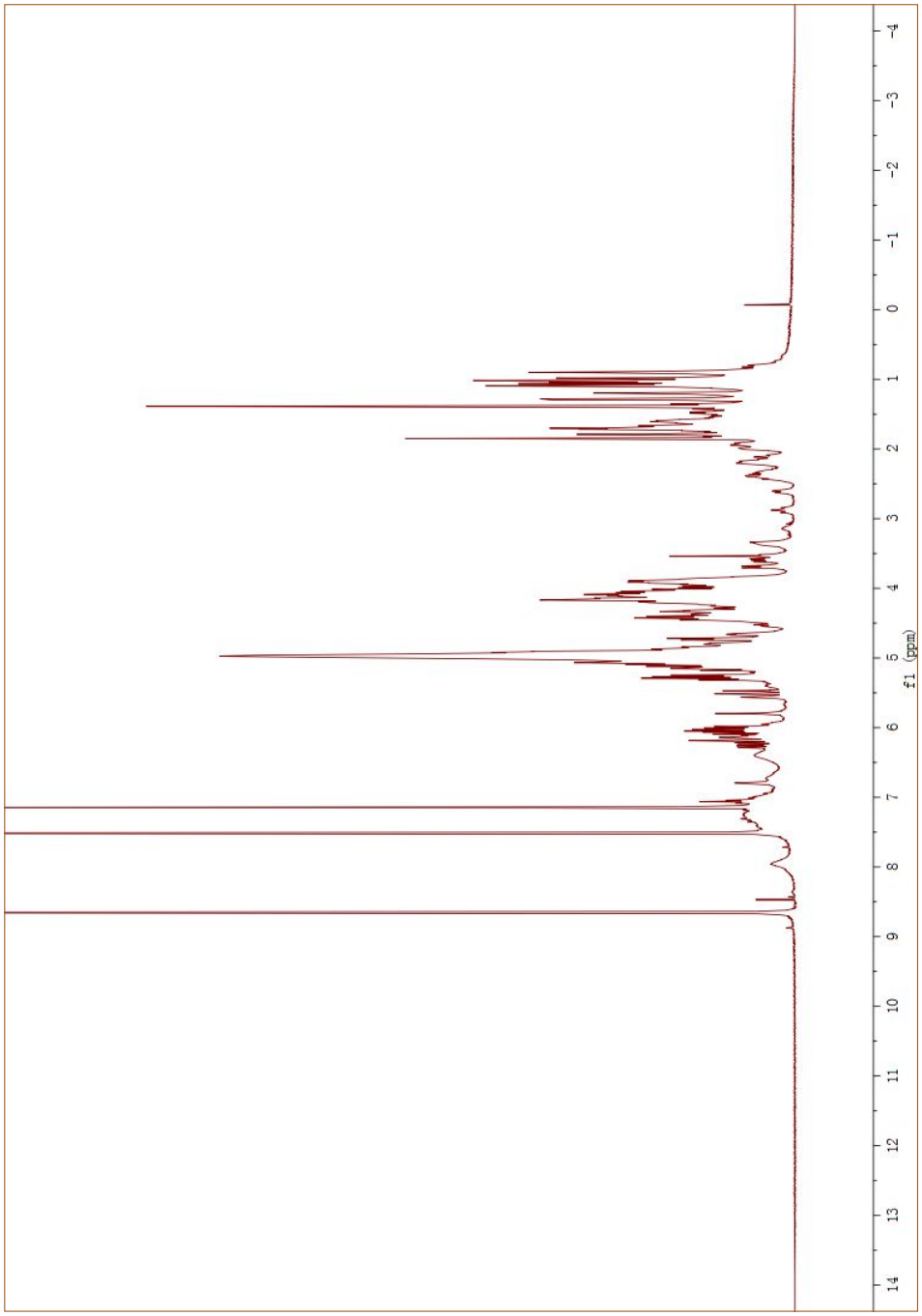

S13. ^{13}C NMR spectrum of proceraoside F (**2**)

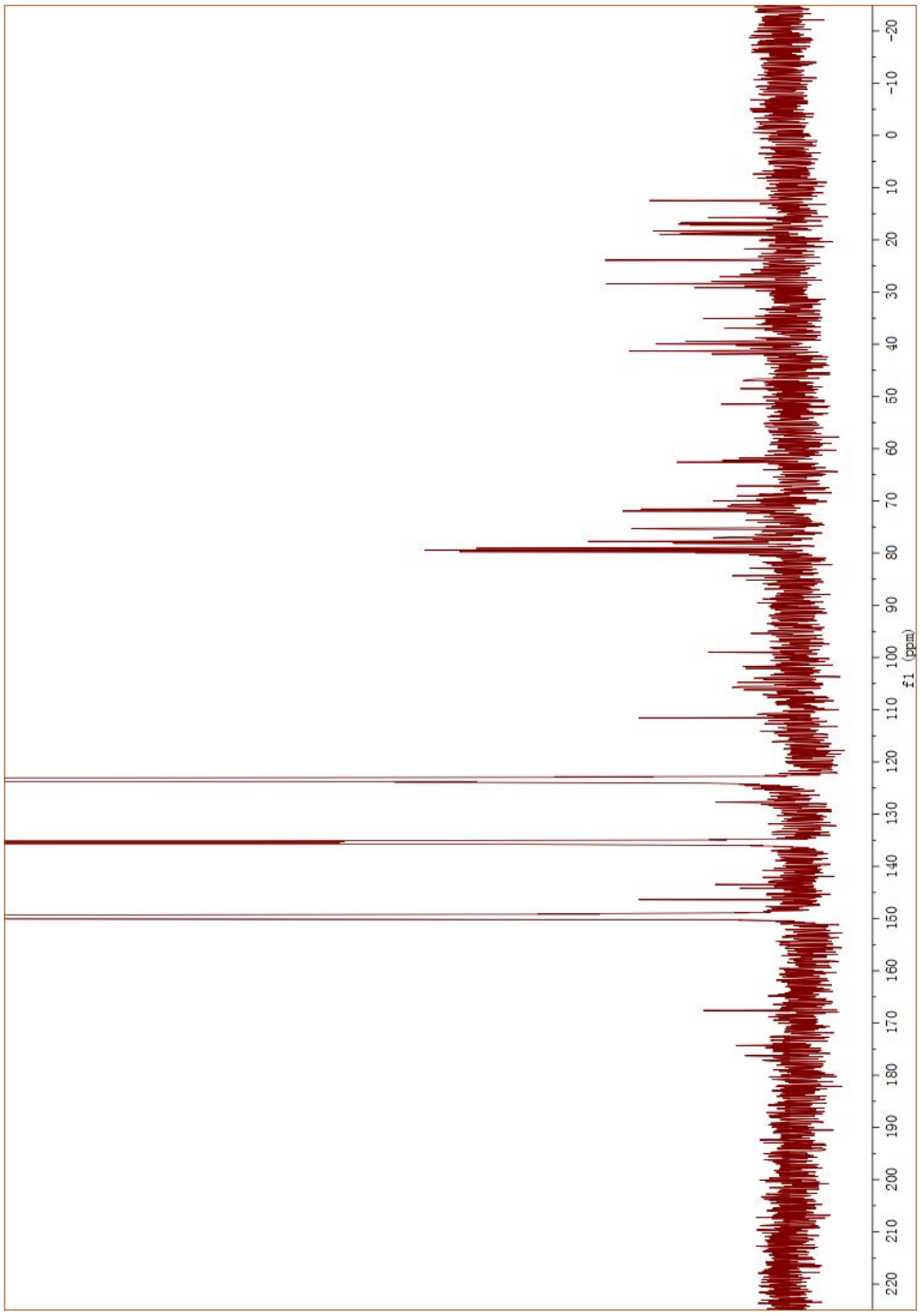

S14. H-H COSY spectrum of proceraoside F (**2**)

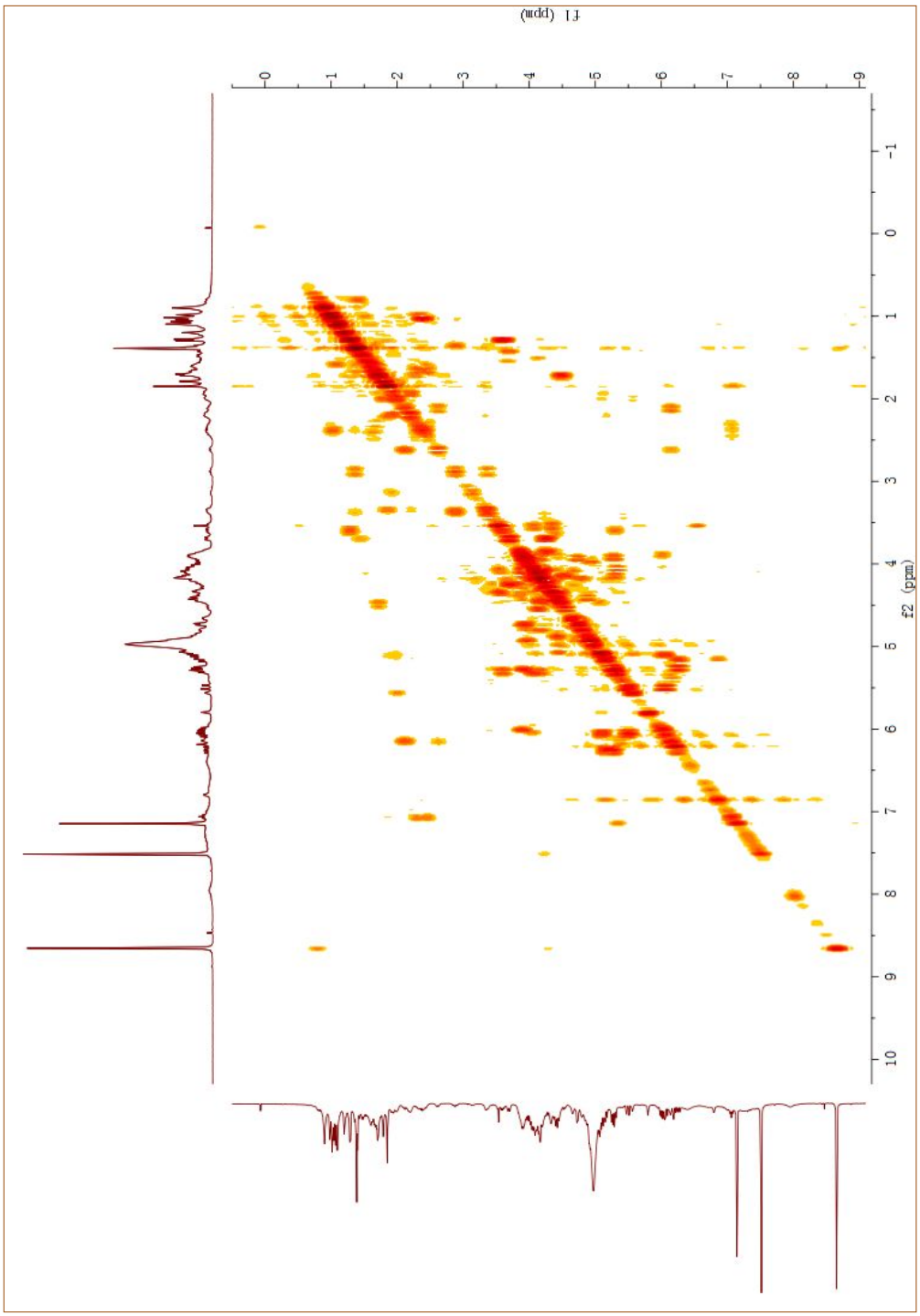

S15. HMQC spectrum of proceraoside F (**2**)

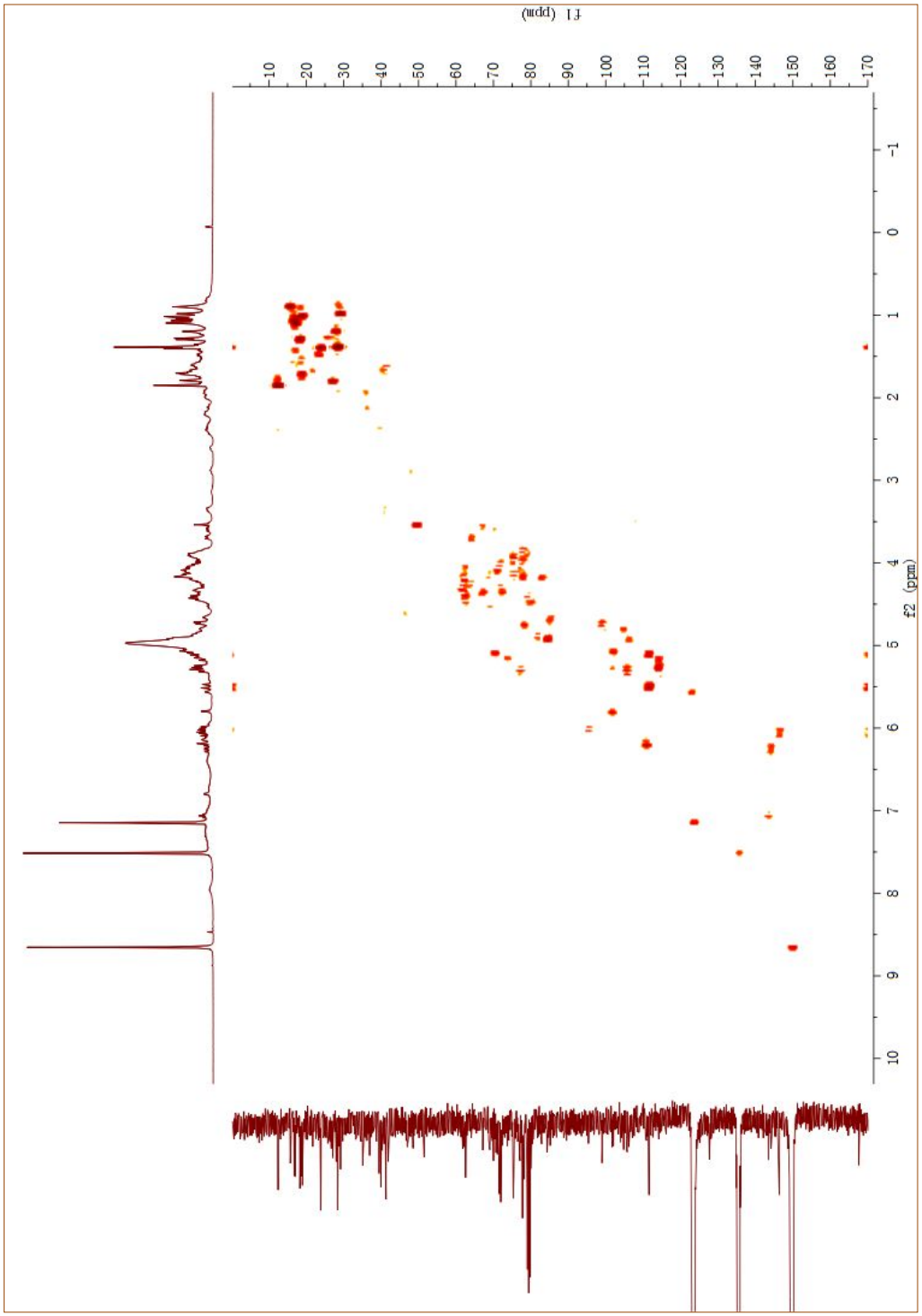

S16. HMBC spectrum of proceraoside F (**2**)

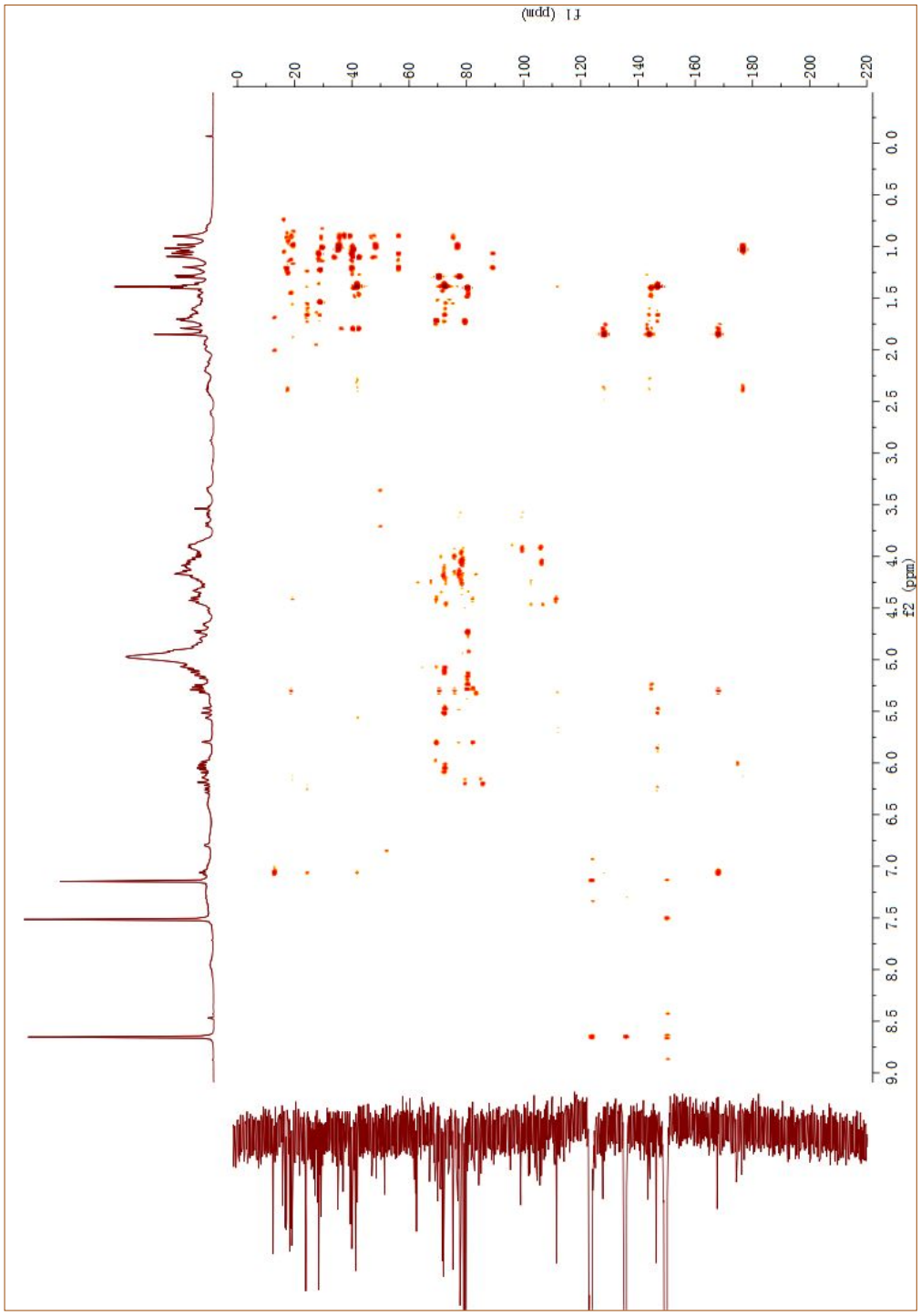

S17. NOSEY spectrum of proceraoside F (**2**)

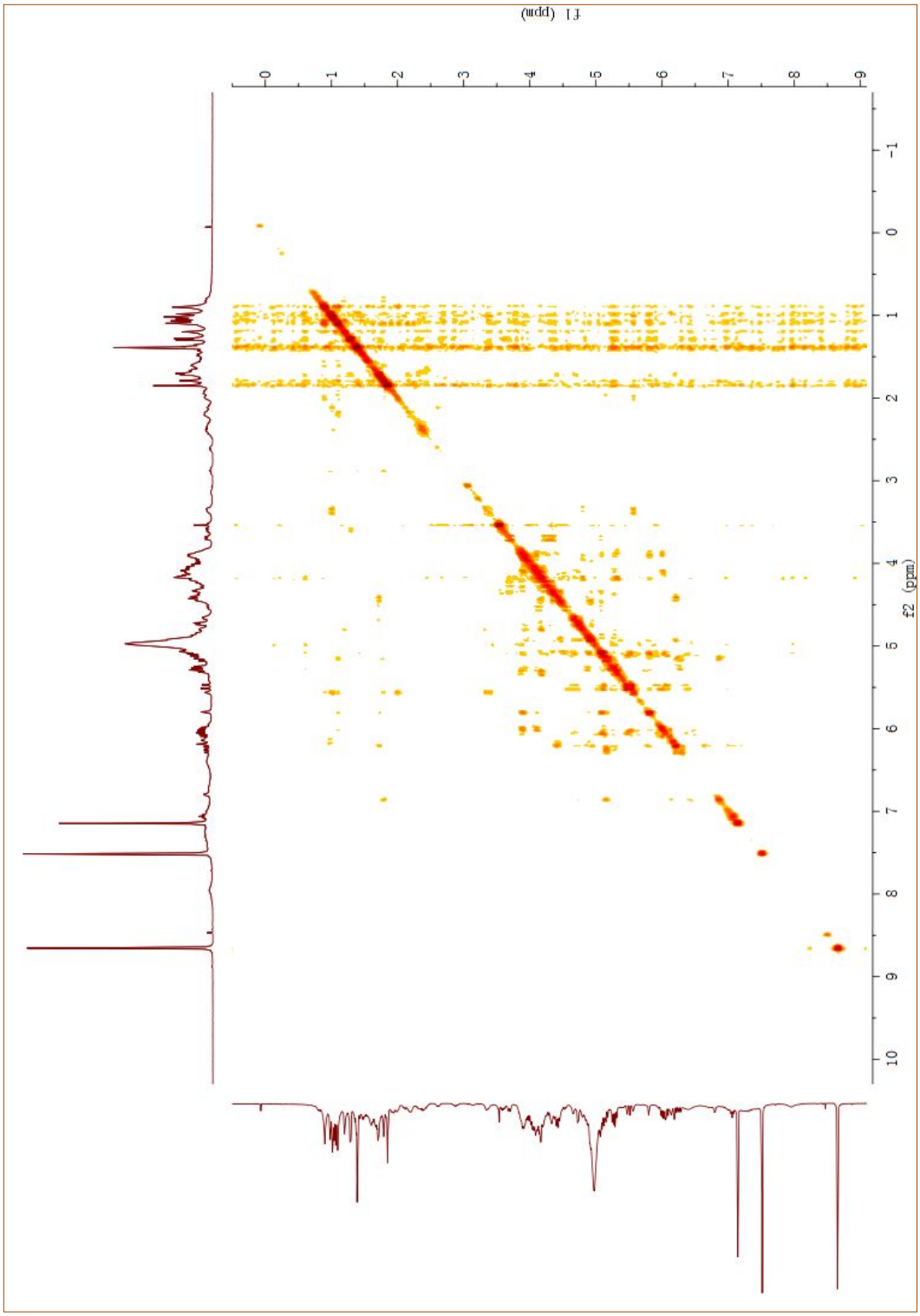

S18. HRESIMS spectrum of proceraoside F (**2**)

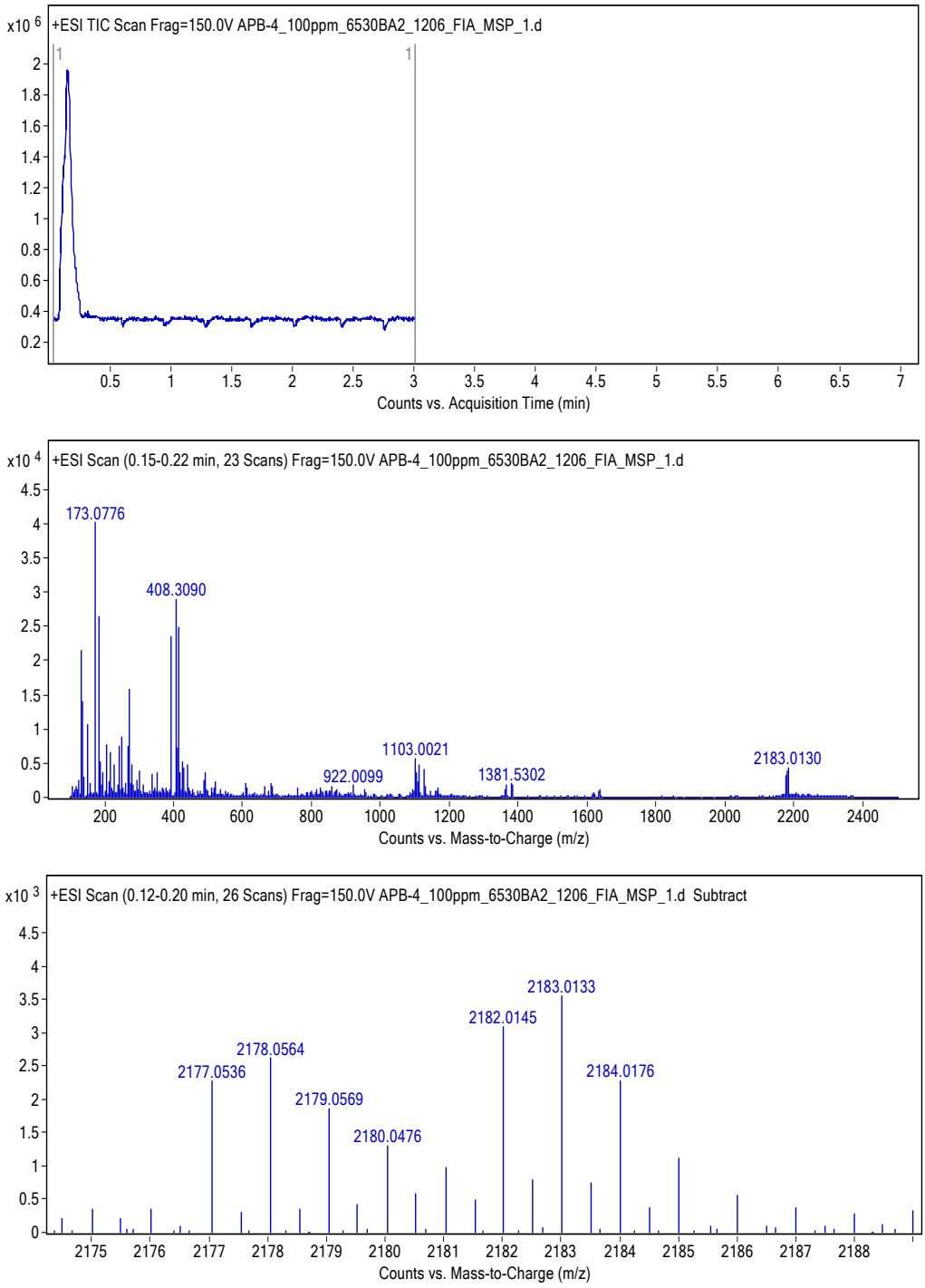

S19. IR spectrum of proceraoside G (**3**)

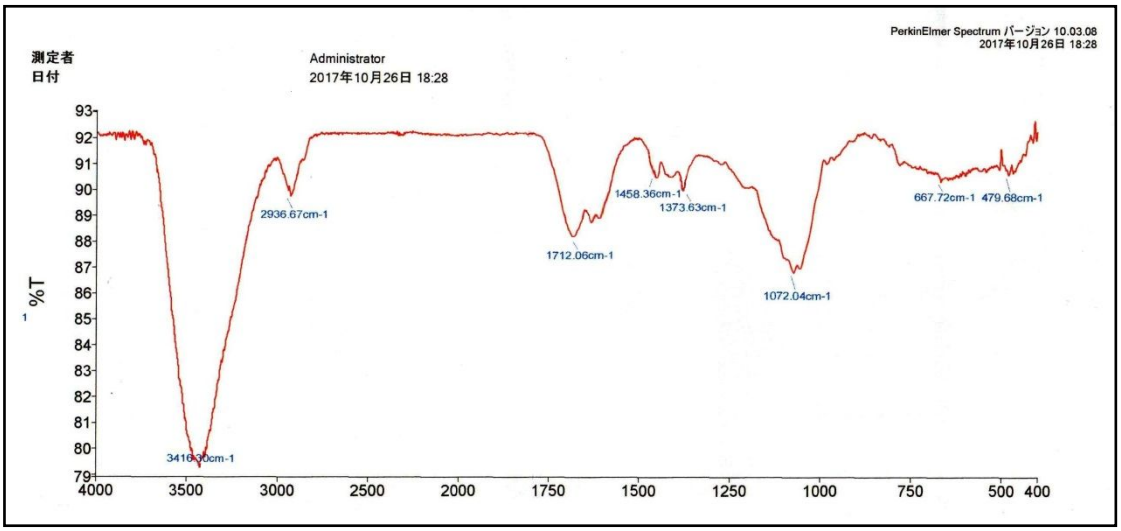

S20. UV spectrum of proceraoside G (**3**)

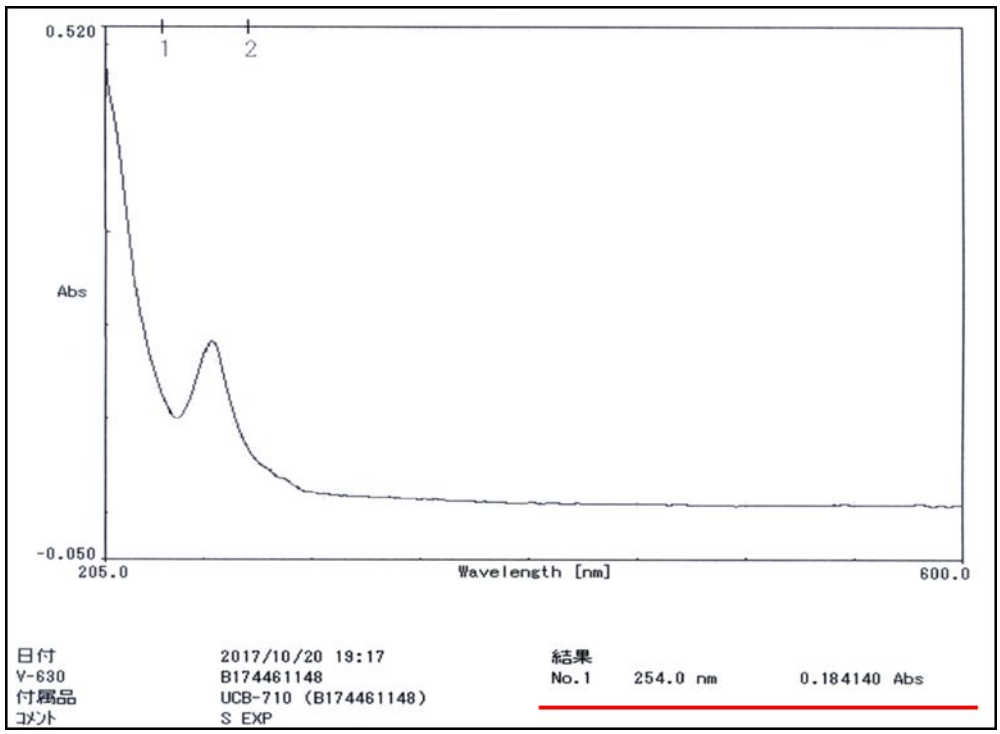

S21. ^{1}H NMR spectrum of proceraoside G (**3**)

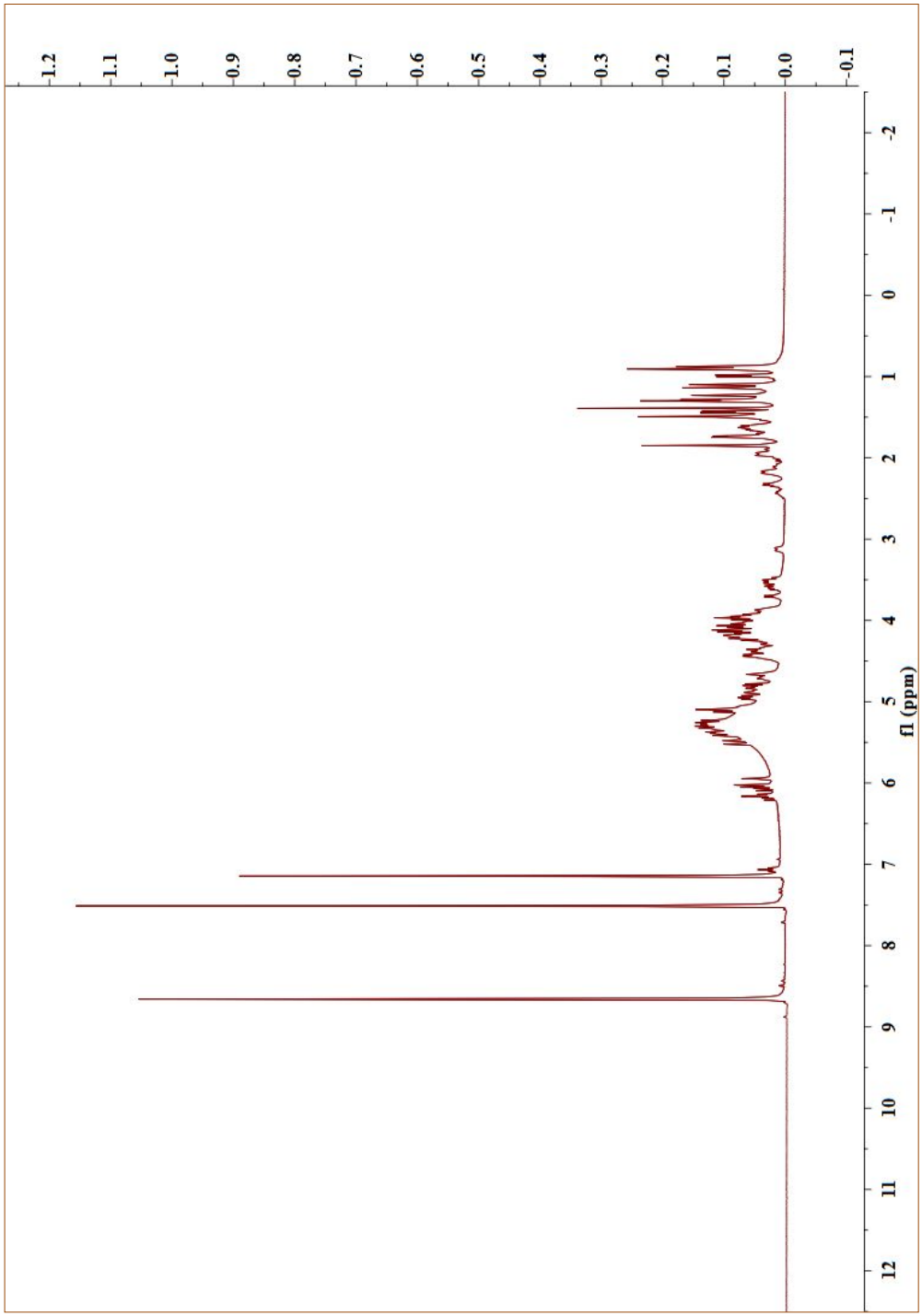
1.2
1.1
1.0
0.9
0.8
0.7
0.6
0.5
0.4
0.3
0.2
0.1
0.0
-0.1
12
11
10
9
8
7
6
5
4
3
2
1
0
-1
-2
f1 (ppm)

S22 ^{13}C NMR spectrum of proceraoside G (**3**)

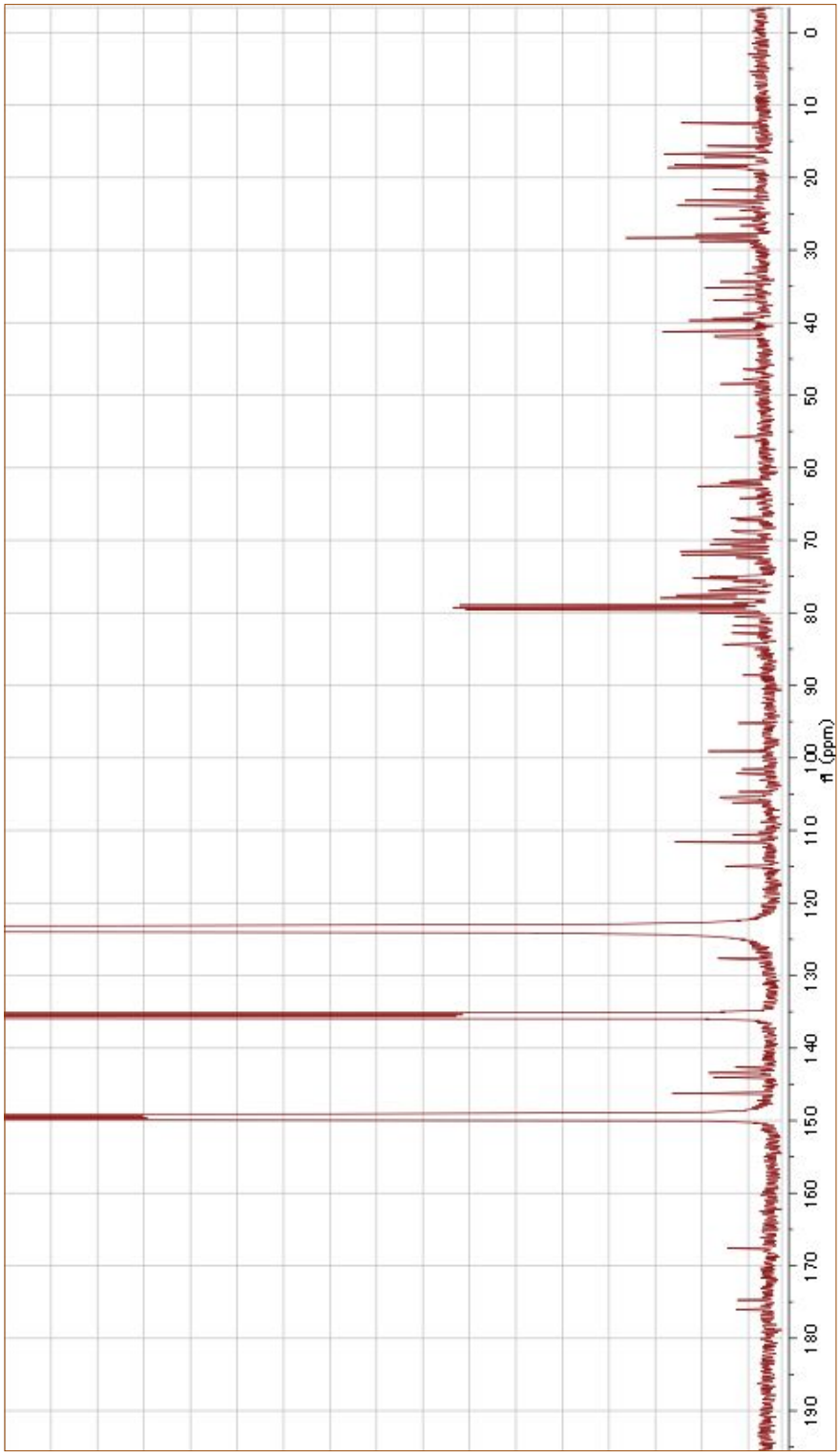

S23. HMQC spectrum of proceraoside G (**3**)

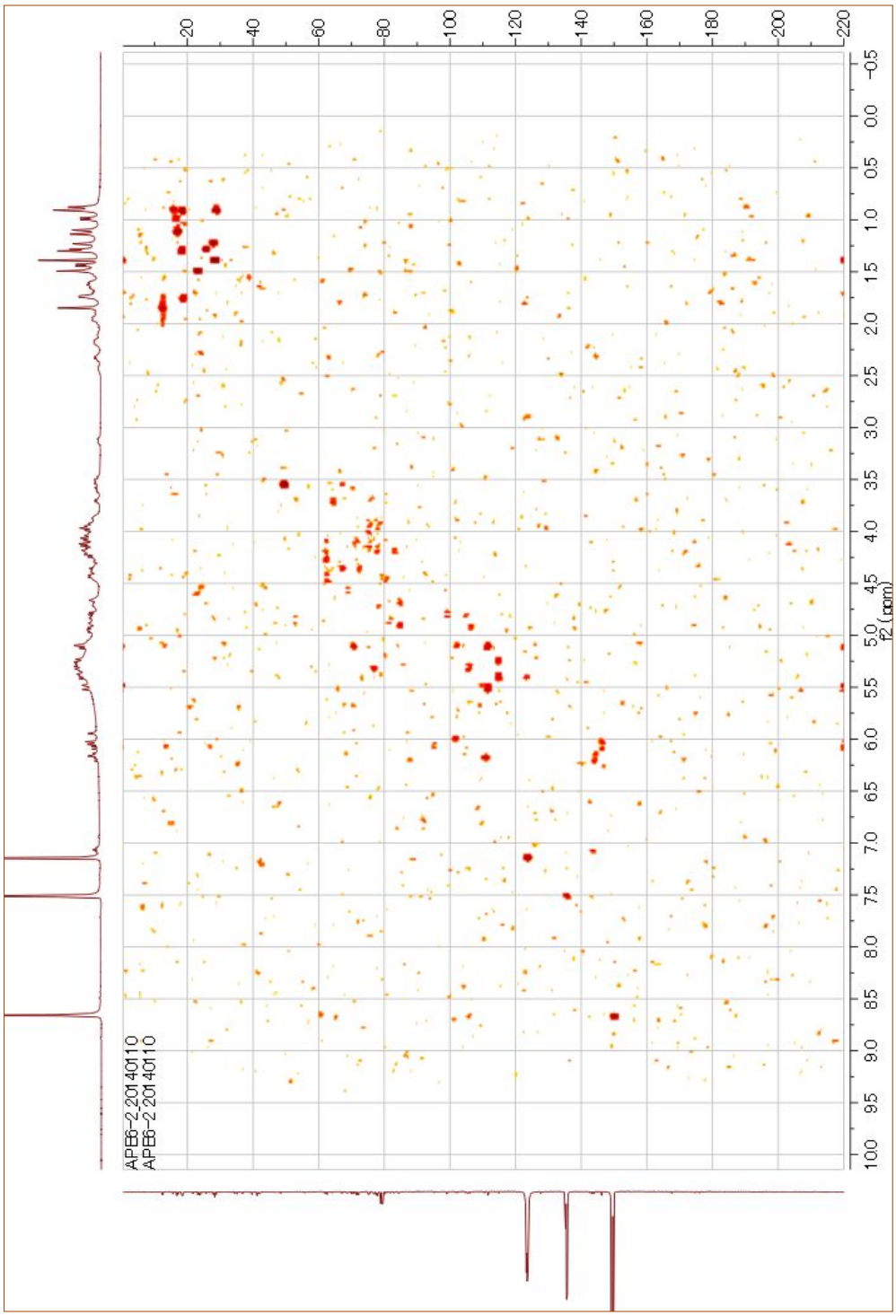

S24. HMBC spectrum of proceraoside G (**3**)

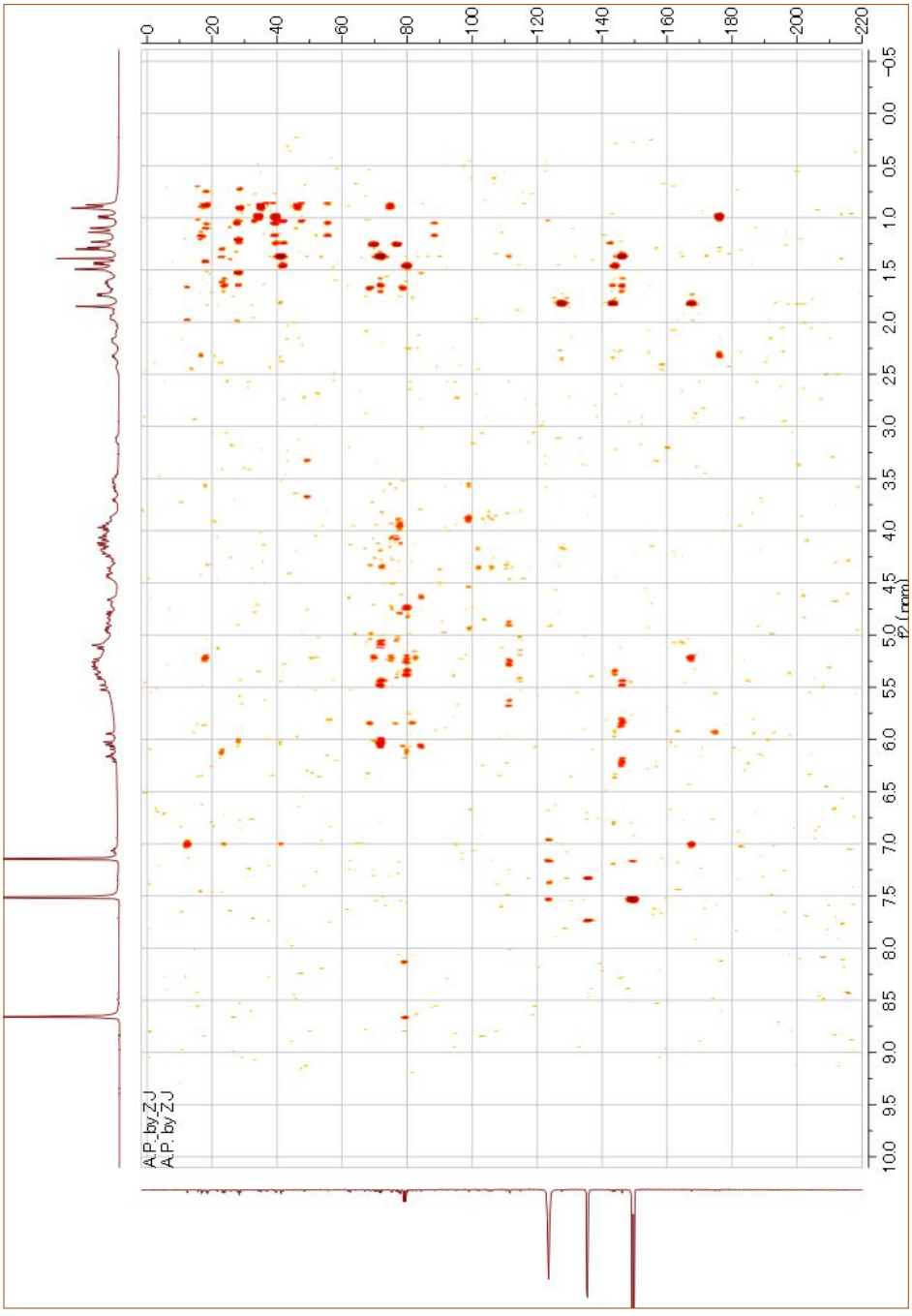

S25. HRESIMS spectrum of proceraoside G (**3**)

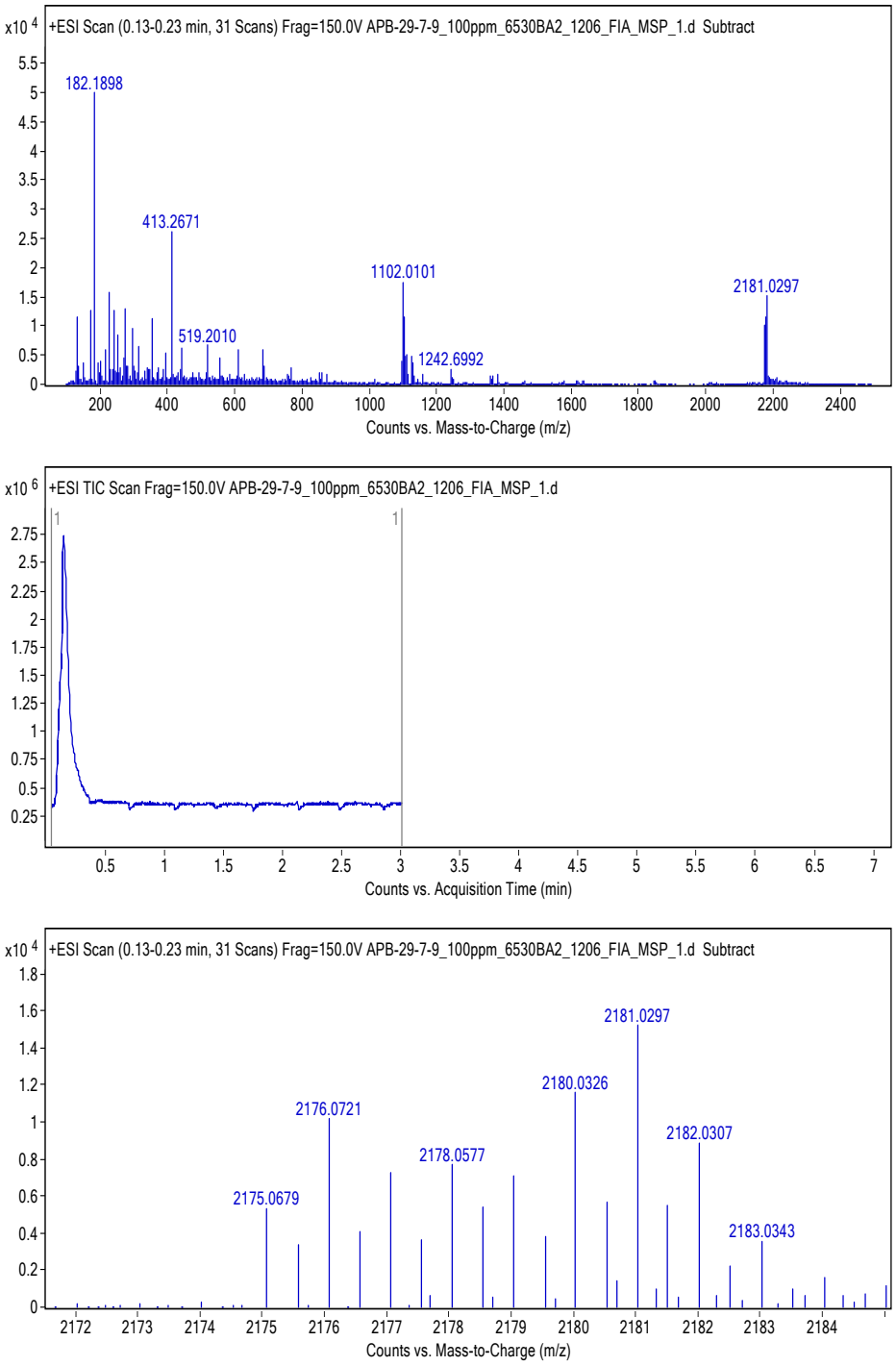

S26. Sample preparation and experimental conditions used for GLC analysis

S26.1. Synthetise of monosaccharide derivative

Authentic samples of monosaccharide (glucose, rhamnose, arabinose, xylose, fucose, quinovose, each 5.0 mg) and L-cysteine methyl ester hydrochloride (7.0 mg) was dissolved in pyridine (0.7 ml) and heated at 60 °C for 1.0 h, and then TMS-HT (0.5 ml) was added to the mixture and heated at 60 °C for 0.3 h to afford their trimethylsiyl thiazolidine derivatives (Fig S1). The reaction mixture was centrifuged, and the supernatant (1.0 ml) was then subjected to GLC analysis for the identification of authentic samples [1].

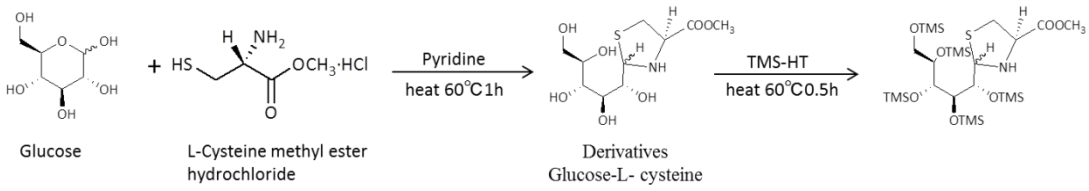

Fig S1. Synthetise of monosaccharide derivative

S26.2. GLC analysis of samples of each monosaccharide derivative

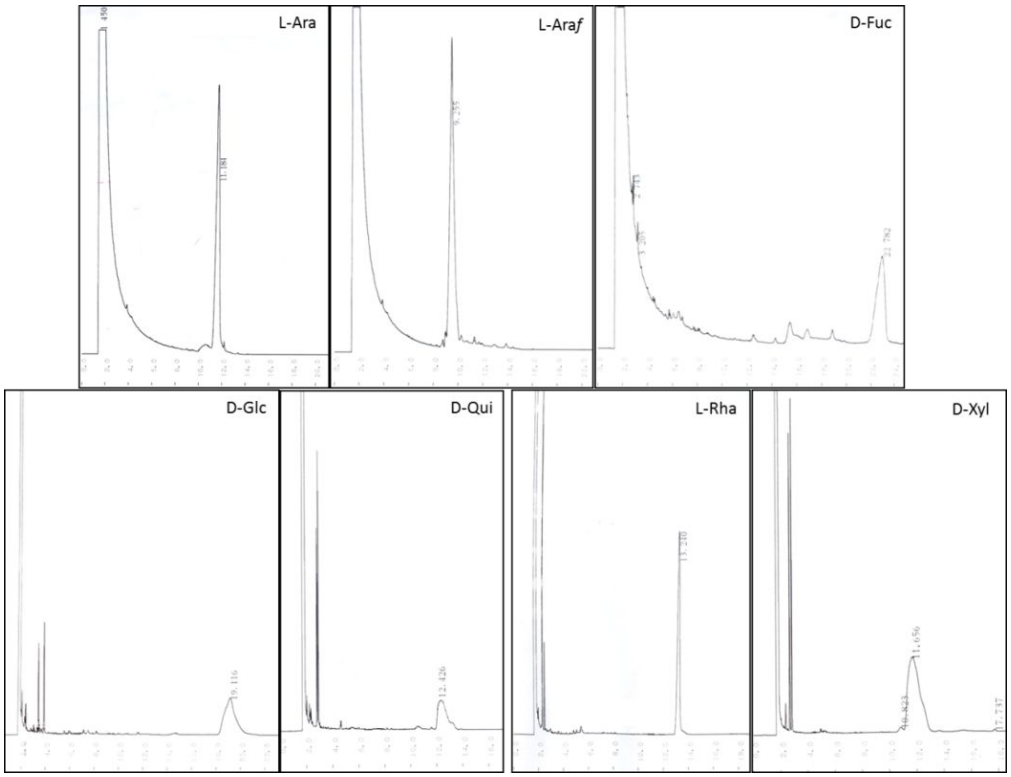

Fig S2. GLC analysis of samples of each monosaccharide derivative

Table S1. Retention time of trimethylsiyl thiazolidine derivatives

Monosaccharide	Configuration	t_R (min)[a]
Arabinose	L	11.336 ± 0.612
Arabinofuranose	L	9.255 ± 0.521
Fucose	D	22.472 ± 0.812
Glucose	D	19.216 ± 0.618
Quinovose	D	12.158 ± 0.661
Rhamnose	L	13.334 ± 0.516
Xylose	D	11.575 ± 0.654

[a] Mean values of three determinations

GLC conditions: Equipment: SHIMADZU GC-2014; column: Agilent J&W DB-17, 30 m × 0.32 mm

(i.d.); column temp: 200 ℃; injector temp: 270 ℃; injector mode: SPLIT; detector temp: 270 ℃; detector: FID; He flow rate: 0.5 ml/min. The results were displayed in Fig S2 and Table S1.

S26.3. Acid Hydrolysis of compounds

A solution of each compound (3.0 mg) in H_2O (2.0 mL) and 2 M aq. CF_3COOH (11.0 mL) was heated under reflux in water bath for 2 h. The mixture was diluted with H_2O and extracted with AcOEt (3×). The H_2O layer was concentrated to dryness by adding repeatedly MeOH to remove acid, and the residue was subjected to TLC with using a mixture of $CHCl_3$-MeOH-AcOH-H_2O (60:32:12:8) as the eluant, which afforded monosaccharide spots. Then, the residues were derivatived to their trimethylsiyl thiazolidine derivatives. The mixture was centrifuged, and a portion (1 μL) of the filtrate was subjected to GLC analysis.[2] The GLC afforded two peaks with t_R values of 9.255, 11.336, 11.575, 12.158, 13.334, 19.216 and 22.475 min, which were identical with those of authentic L-arabinofuranose, L-arabinose, D-xylose, D-quinovose, L-rhamnose, D-glucose, and D-fucose, compatible with those of authentic samples (Fig S3).

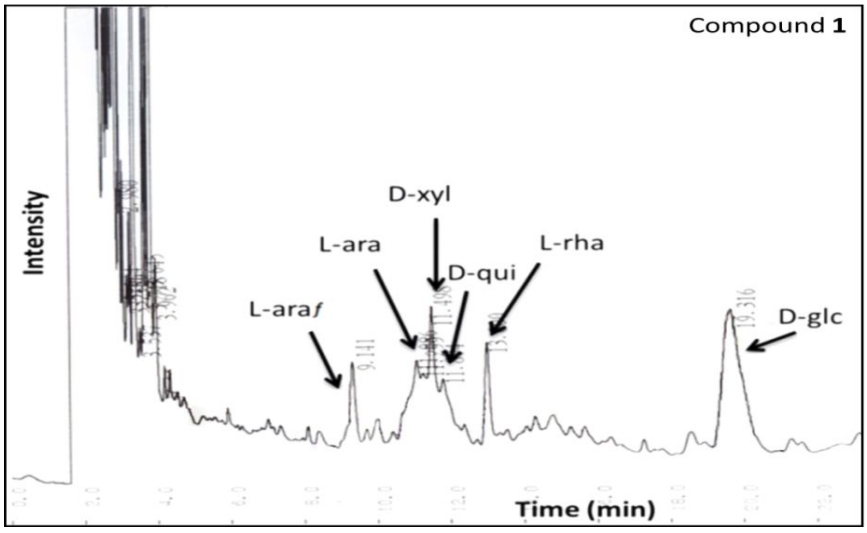

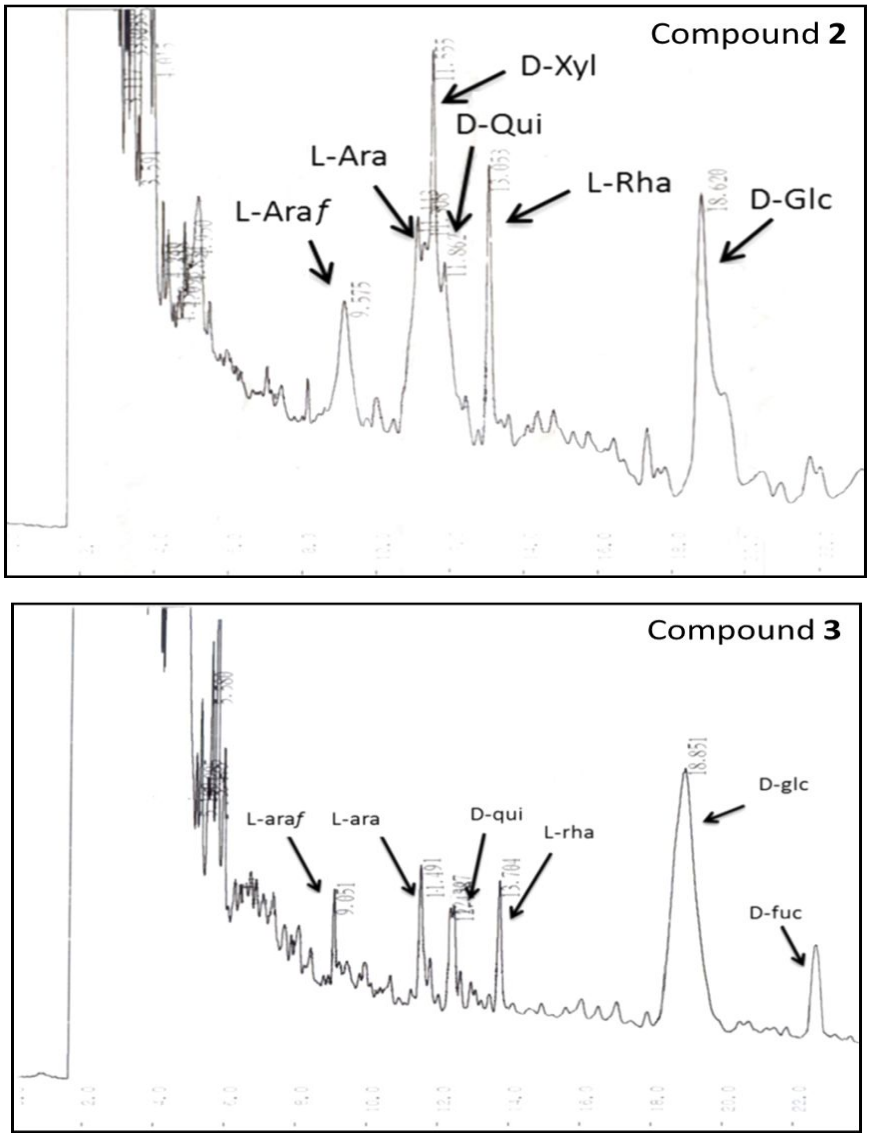

Fig. S3 GLC analysis of monosaccharide derivatives from compounds

References:

[1] M. Elbandy, T. Miyamoto, C. Delaude, M. A. Lacaile-Dubois, J. Nat. Prod. 66, 1154 (2003).

[2] S. Hara, et al., Chem. Pharm. Bull. 35, 501 (1987).

S27. The LC-MS/MS analysis of **1-3**

S27.1. Gradient chromatographic condition

HPLC analysis was performed on an Agilent 1200 series with a quaternary pump, vacuum degasser, auto sampler, column heater–cooler. r. Samples were separated on ZORBAX eclipse Plus C18 (2.1 x 100 mm, 1.8 μm). The column temperature was set at 40 ℃. The mobile phase consisted of 5 mM CH3COONH4 aq. (A) and acetonitrile (B). The gradient elution program was as follows: 5→65→90 →90 (B) at 0-10-10.1-15 min, respectively. The flow rate was 0.3 mL/min and the sample volume injected was 5 μL.

S27.2. HPLC-Q-TOF-MS analysis

The HPLC system was interfaced to an Agilent 6530 LC/QTOF (Agilent Technologies, Santa Clara, USA) TOF mass spectrometer equipped with an electrospray interface operating under the chromatographic conditions mentioned above. The optimized MS operating conditions were as follows: negative and positive ionization mode, scan spectra from m/z 100 to 2000, drying gas (N2) flow rate of 10.0 L/min, drying gas temperature of 350 ℃, nebulizer pressure of 50 psi, and fragmentor voltage of 150 V. Data were processed using MassHunter Qualitative Analysis B.04.00 (Agilent Technologies).

Compound **1** MSMS (Positive-ion mode)

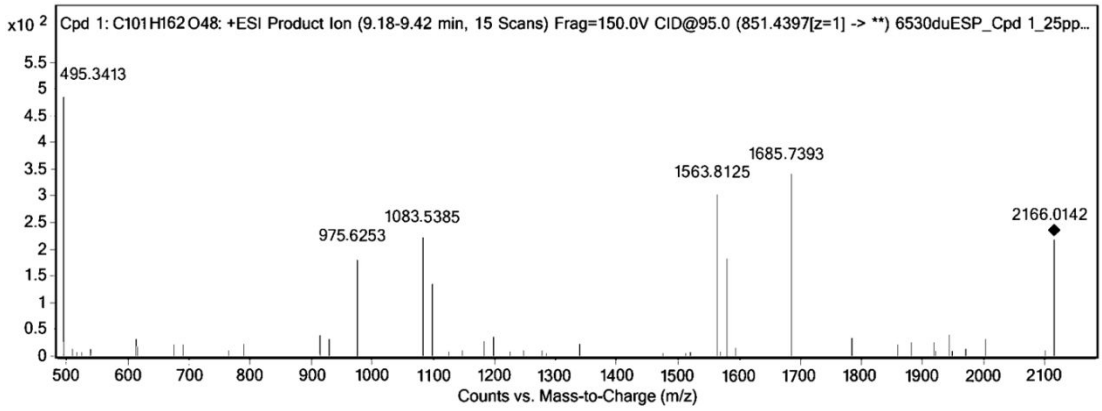

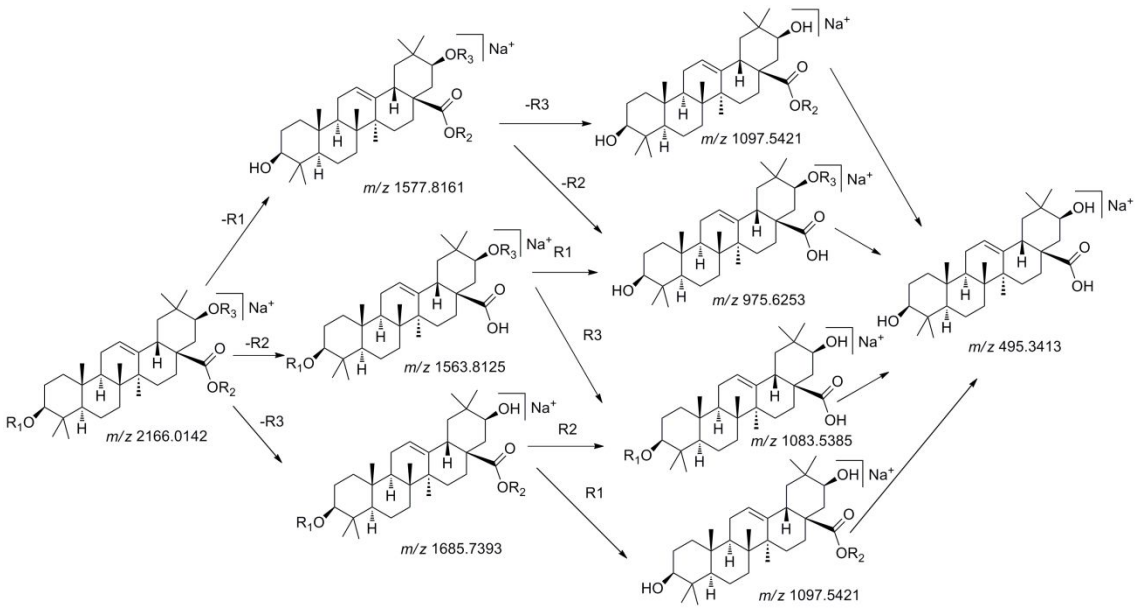

The provide fragmentation pathway of compound **1**. R_1 = -Xyl-Ara-Glc_1-Glc_2; R_2 = Glc_4-Ara*f*-Rha-Glc_3; R_3 = -MA_2-Qui-MA_1.

HRESIMS *m/z*: 2166.0142 $[M + Na]^+$ (calcd for $C_{101}H_{162}O_{48}$ Na, 2166.0133).

m/z 1685.7393; $C_{75}H_{122}NaO_{40}$; Calc. 1685.7405
$[(M+Na)-166-146-168]^+$;
$[(M+Na)-MA_2-Qui-MA_1]^+$;

m/z 1577.8161; $C_{79}H_{126}NaO_{30}$; Calc. 1577.8292
$[(M+Na)-(2\times132)-(2\times162)]^+$;
$[(M+Na)$-Xyl-Ara-Glc_1-$Glc_2]^+$;

m/z 1563.8125; $C_{78}H_{124}NaO_{30}$; Calc. 1563.8141
$[(M+Na)-(2\times162)-132-146]^+$;
$[(M+Na)-Glc_4$-Ara*f*-Rha-$Glc_3]^+$;

m/z 1097.5421; $C_{53}H_{86}NaO_{22}$; Calc. 1097.5528
$[(M+Na)-(2\times132)-(2\times162)-166-146-168]^+$;
$[(M+Na)-$ Xyl-Ara-Glc_1-Glc_2-MA_2-Qui-$MA_1]^+$;

m/z 1083.5385; $C_{52}H_{84}NaO_{22}$; Calc. 1083.5375

$[(M+Na)-(2\times162)-132-(2\times146)-166-168]^+$;

$[(M+Na)-Glc_4-Ara\textit{f}-Rha-Glc_3-MA_2-Qui-MA_1]^+$;

m/z 975.6253; $C_{56}H_{88}NaO_{12}$; Calc. 975.6263

$[(M+Na)-(3\times132)-(4\times162)-146]^+$;

$[(M+Na)-Xyl-Ara-Glc_1-Glc_2-Glc_4-Ara\textit{f}-Rha-Glc_3]^+$;

m/z 495.3413; $C_{30}H_{48}NaO_4$; Calc. 495.3497

$[(M+Na)-(3\times132)-(4\times162)-(2\times146)-166-168]^+$;

$[(M+Na)-Xyl-Ara-Glc_1-Glc_2-Glc_4-Ara\textit{f}-Rha-Glc_3-MA_2-Qui-MA_1]^+$;

Compound **2** MSMS (Positive-ion mode)

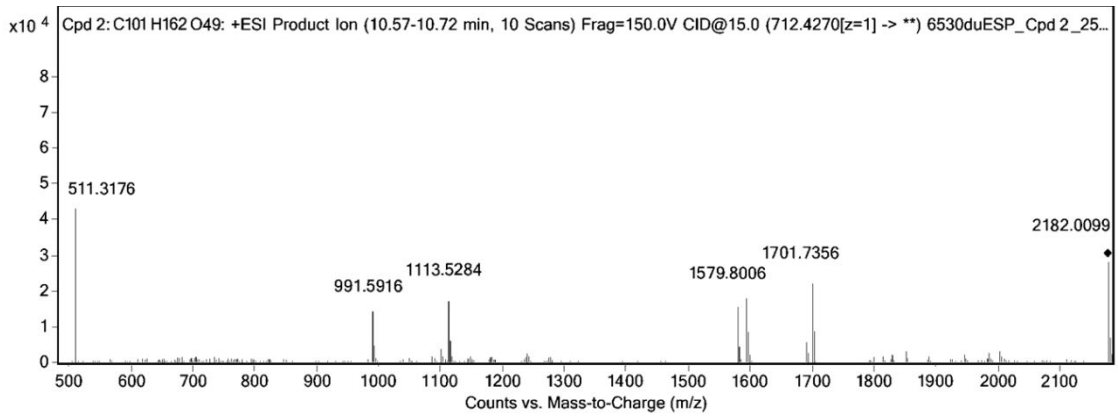

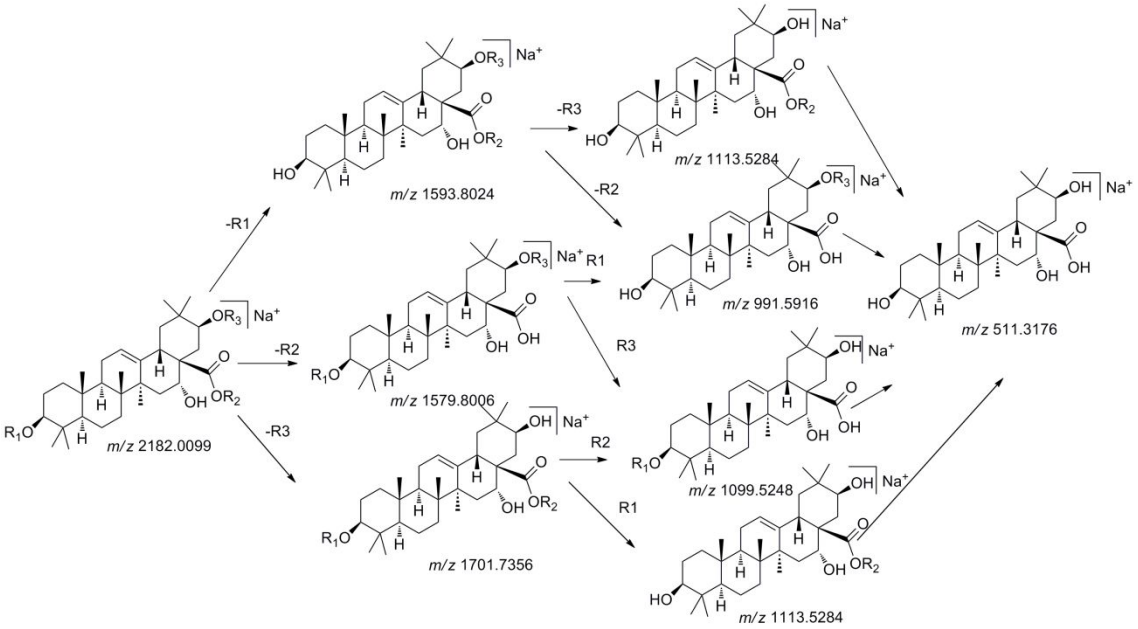

The provide fragmentation pathway of compound **2**. R_1=-Xyl-Ara-Glc_1-Glc_2; R_2= Glc_4-Ara*f*-Rha-Glc_3; R_3=-MA_2-Qui-MA_1.

HRESIMS *m/z*: 2182.0099 $[M + Na]^+$ (calcd for $C_{101}H_{162}O_{49}$ Na, 2182.0082).

m/z 1701.7356; $C_{75}H_{122}NaO_{41}$; Calc. 1701.7351

$[(M+Na)-166-146-168]^+$;

$[(M+Na)-MA_2-Qui-MA_1]^+$;

m/z 1593.8024; $C_{79}H_{126}NaO_{31}$; Calc. 1593.8241

$[(M+Na)-(2\times132)-(2\times162)]^+$;

$[(M+Na)$-Xyl-Ara-Glc_1-$Glc_2]^+$;

m/z 1579.8006; $C_{78}H_{124}NaO_{31}$; Calc. 1579.8086

$[(M+Na)-(2\times162)$ -132-146$]^+$;

$[(M+Na)$-Glc_4-Ara*f*-Rha-$Glc_3]^+$;

m/z 1113.5284; $C_{53}H_{86}NaO_{23}$; Calc. 1113.5475

$[(M+Na)-(2\times132)-(2\times162)$-166-146-168$]^+$;

$[(M+Na)$- Xyl-Ara-Glc_1-Glc_2-MA_2-Qui-$MA_1]^+$;

m/z 1099.5248; $C_{52}H_{84}NaO_{23}$; Calc. 1099.5320

$[(M+Na)-(2\times162)$ -132-(2×146)-166-168$]^+$;

$[(M+Na)$-Glc_4-Ara*f*-Rha-Glc_3-MA_2-Qui-$MA_1]^+$;

m/z 991.5916; $C_{56}H_{88}NaO_{13}$; Calc. 991.6210

$[(M+Na)-(3\times132)-(4\times162)-146]^+$;

$[(M+Na)$-Xyl-Ara-Glc_1-Glc_2 -Glc_4-Ara*f*-Rha-$Glc_3]^+$;

m/z 511.3176; $C_{30}H_{48}NaO_5$; Calc. 511.3443

$[(M+Na)-(3\times132)-(4\times162)-(2\times146)$-166-168$]^+$;

$[(M+Na)$-Xyl-Ara-Glc_1-Glc_2-Glc_4-Ara*f*-Rha-Glc_3-MA_2-Qui-$MA_1]^+$;

Compound **3** MSMS (Positive-ion mode)

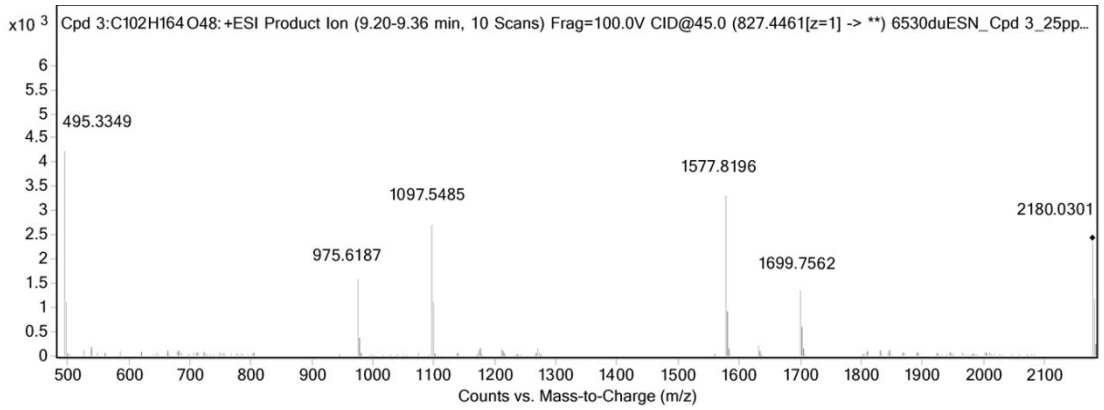

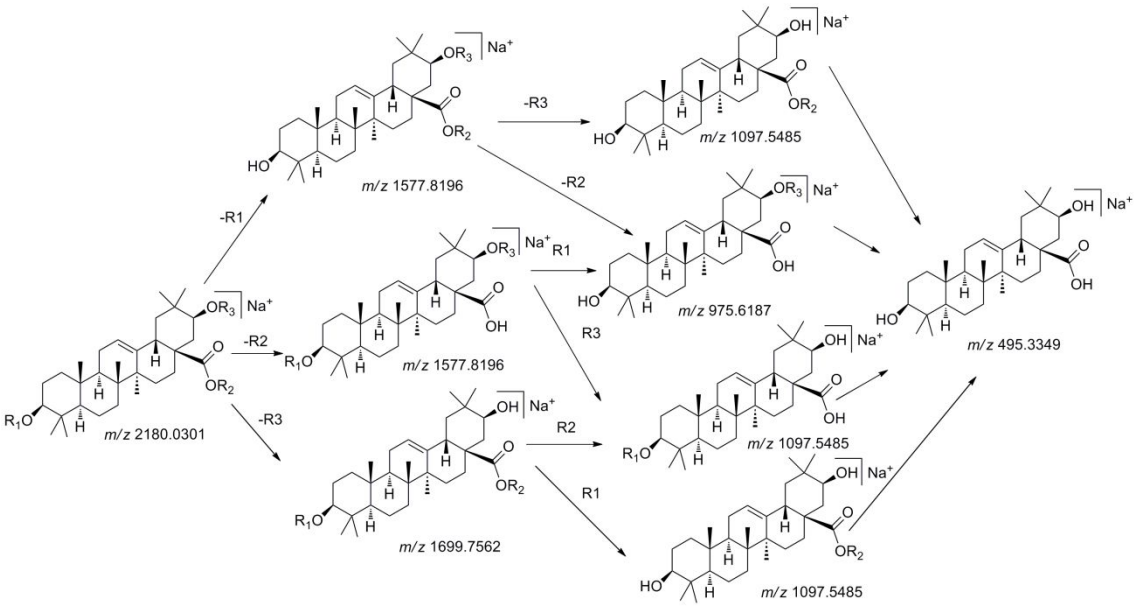

The provide fragmentation pathway of compound **3**. R_1 = -Xyl-Fuc-Glc_1-Glc_2; R_2 = Glc_4-Ara*f*-Rha-Glc_3; R_3 = -MA_2-Qui-MA_1.

HRESIMS *m/z*: 2180.0301 $[M + Na]^+$ (calcd for $C_{102}H_{164}O_{48}$ Na, 2180.0290).

m/z 1699.7562; $C_{76}H_{124}NaO_{40}$; Calc. 1699.7560

$[(M+Na)-166-146-168]^+$;

$[(M+Na)-MA_2-Qui-MA_1]^+$;

m/z 1577.8196; $C_{79}H_{126}NaO_{30}$; Calc. 1577.8295

[(M+Na)-132-146-(2×162)]$^{+}$;
[(M+Na)-Xyl-Fuc-Glc$_1$-Glc$_2$]$^{+}$;
Or [(M+Na)-Glc$_4$-Ara*f*-Rha-Glc$_3$]$^{+}$;

m/z 1097.5485; $C_{53}H_{86}NaO_{22}$; Calc. 1079.5528
[(M+Na)-132-(2×162)-166-(2×146)-168]$^{+}$;
[(M+Na)- Xyl-Fuc-Glc$_1$-Glc$_2$-MA$_2$-Qui-MA$_1$]$^{+}$;
Or [(M+Na)-Glc$_4$-Ara*f*-Rha-Glc$_3$-MA$_2$-Qui-MA$_1$]$^{+}$;

m/z 975.6187; $C_{56}H_{88}NaO_{12}$; Calc. 975.6263
[(M+Na)-(2×132)-(4×162)-(2×146)]$^{+}$;
[(M+Na)-Xyl-Fuc-Glc$_1$-Glc$_2$ -Glc$_4$-Ara*f*-Rha-Glc$_3$]$^{+}$;

m/z 495.3349; $C_{30}H_{48}NaO_4$; Calc. 495.3497
[(M+Na)-(2×132)-(4×162)-(3×146)-166-168] $^{+}$;
[(M+Na)-Xyl-Fuc-Glc$_1$-Glc$_2$-Glc$_4$-Ara*f*-Rha-Glc$_3$-MA$_2$-Qui-MA$_1$]$^{+}$;

S 28. Melanogenesis-inhibitory activties[a] of *A. procera* extracts

Extract or fraction	Melanin content (%)		Cell viability (%)	
	10 μg ml^{-1}	100 μg ml^{-1}	10 μg ml^{-1}	100 μg ml^{-1}
Control (100% DMSO)	100.0 ± 4.2	100.0 ± 4.0	100.0 ± 2.1	100.0 ± 3.0
Hexane extract	92.0 ± 2.7	19.0 ± 2.6	100.2 ± 2.1	54.7 ± 2.2
MeOH extract	46.7 ± 5.2	4.9 ± 0.5	73.0 ± 4.1	38.4 ± 3.0
EtOAc fraction	104.3 ± 3.0	19.4 ± 1.5	97.4 ± 6.6	24.8 ± 1.4
BuOH fraction	2.9 ± 0.2	7.5 ± 0.4	3.0 ± 1.2	1.0 ± 0.4
H_2O fraction	108.4 ± 2.8	30.0 ± 0.4	118.9 ± 3.2	34.7 ± 0.9
Arbutin[b]	98.7 ± 9.7	68.9 ± 2.3	96.5 ± 2.9	87.1 ± 2.8

[a] Melanin content and cell viability were determined based on the absorbances at 405, and 570 (test wavelength)–630 (reference wavelength) nm, respectively, by comparison with those for DMSO (100%). Each value represents the mean ± S.D. (n = 3). Concentration of DMSO in the sample solution was 2 μl·ml^{-1}. [b] Positive control.

S 29. Cytotoxic activities of *A. procera* extracts in human cancer cell lines

Extract or fraction	Cell lines, IC_{50} (Mean ± SD, μg·ml^{-1})[a]							
	HL60	AZ521	SKBR3	KB	HeLa	HT29	HepG2	A549
Hexane extract	69.9 ± 3.3	> 100	> 100	12.5 ± 1.7	84.5 ± 9.1	21.4 ± 3.2	36.9 ± 3.9	>100
MeOH extract	89.7 ± 5.0	> 100	> 100	37.1	29.8 ± 2.8	42.5 ± 3.4	> 100	>100
AcOEt fraction	>100	> 100	> 100	> 100	ND[b]	ND[b]	ND[b]	>100
BuOH fraction	4.1 ± 1.2	> 100	> 100	8.7 ± 2.9	5.4 ± 1.5	3.2 ± 1.1	20.5 ± 2.8	11.5 ± 3.8
H_2O fraction	>100	> 100	> 100	> 100	> 100	> 100	80.6 ± 7.1	>100
Cisplatin[c]	1.3 ± 0.3	2.9 ± 0.5	5.6 ± 0.2	3.3 ± 0.1	3.4 ± 1.9	1.1 ± 0.6	5.5 ± 0.7	5.5 ± 0.6

[a] IC_{50} Value was obtained on the basis of triplicate assay results. [b] ND: not determined. [c] positive control.